ERDC/ITL TR-17-2

Information and Technology Laboratory

US Army Corps
of Engineers®
Engineer Research and
Development Center

ERDC
INNOVATIVE SOLUTIONS
for a safer, better world

Navigation Systems Research Program

A Systematic Approach for Determining Vertical Pile Depth of Embedment in Cohesionless Soils to Withstand Lateral Barge Train Impact Loads

Barry C. White and Robert M. Ebeling

January 2017

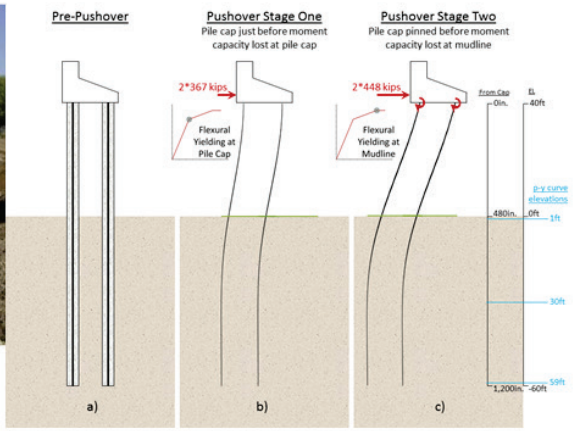

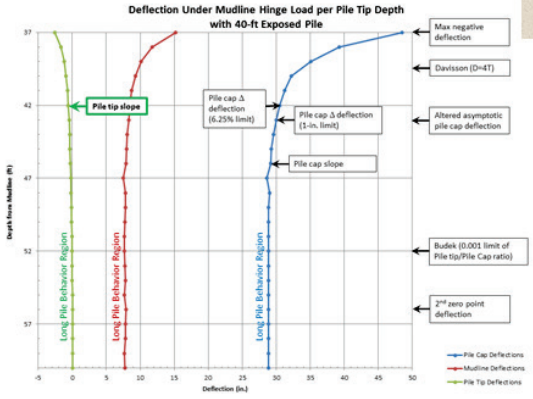

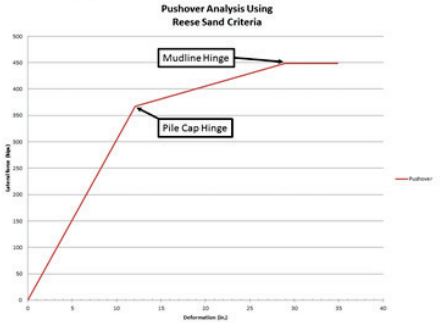

The U.S. Army Engineer Research and Development Center (ERDC) solves the nation's toughest engineering and environmental challenges. ERDC develops innovative solutions in civil and military engineering, geospatial sciences, water resources, and environmental sciences for the Army, the Department of Defense, civilian agencies, and our nation's public good. Find out more at www.erdc.usace.army.mil.

To search for other technical reports published by ERDC, visit the ERDC online library at http://acwc.sdp.sirsi.net/client/default.

Navigation Systems Research Program

ERDC/ITL TR-17-2
January 2017

A Systematic Approach for Determining Vertical Pile Depth of Embedment in Cohesionless Soils to Withstand Lateral Barge Train Impact Loads

Barry C. White and Robert M. Ebeling

Information Technology Laboratory
U.S. Army Engineer Research and Development Center
3909 Halls Ferry Road
Vicksburg, MS 39180-6199

Final report

Prepared for U.S. Army Corps of Engineers
Washington, DC 20314-1000

Under Navigation Systems Research Program, Project number 448769
Work Unit "Flexible Approach Walls"

Abstract

Pile-founded flexible lock approach walls are typically constructed with impact beams simply supported on pile bents or by using an impact deck supported by groups of clustered piles. Cast-in-drilled-hole (CIDH) reinforced concrete (RC) piles have seen recent widespread use as a cost-effective method of transferring superstructure loads to the foundation soil (e.g., cohesionless soils, like sand). The primary design load for lock approach walls are dynamic barge train impacts on a beam or deck, which occur as the barge train aligns itself for entrance to the lock. These bents and decks are supported tens of feet above the mudline and barge impacts occur at the beam or deck level (i.e., lateral loading at approximately the top of the pile). Because of this lateral loading applied at the top of the piles, vertical pile groups must be designed to exhibit long-pile behavior (e.g., nominal change of deflection at the pile cap for a given load as the pile-tip depth of embedment increases). These design loads introduce substantial moments for the vertical piles at a short distance below the mudline. A pushover analysis of vertical-pile clusters can be performed to determine the energy absorption of the structure and the peak loads that cause the piles to hinge a short distance below the mudline, leading to collapse. This peak load is used to compare different pile depth of embedment procedures for long-pile behavior, and leads to the development of a new systematic procedure for defining this depth. Reducing the length of piles will result in a cost savings for Corps projects, especially for in-the-wet construction.

Contents

Figures and Tables

Figures

Tables

Preface

This report was authorized by Headquarters, U.S. Army Corps of Engineers (HQUSACE), and was compiled from April 2014 to December 2014. It was published under the Navigation Systems Research Program, Project number 448769, Work Unit "Flexible Approach Walls." Jeff McKee was the HQUSACE Navigation Business Line Manager.

The Program Manager for the Navigation Systems Research Program was Charles Wiggins, Coastal and Hydraulics Laboratory (CHL), U.S. Army Engineer Research and Development Center (ERDC). Jeff Lillycrop (CHL) was Technical Director. The research was led by Dr. Robert M. Ebeling, Information Technology Laboratory (ITL), under the general supervision of Dr. Reed L. Mosher, Director, ITL; Patti S. Duett, Deputy Director, ITL. This work effort was also conducted under the general supervision of Dr. Jerrell R. Ballard, Computational Science and Engineering Division (CSED), ITL. Ebeling was the Principal Investigator of the "Flexible Approach Walls" work unit.

The authors would like to give a special thanks to Ralph W. Strom, consultant, for the insight and collaborative efforts that he provided on this project. Strom was a key developer of the pushover method of analysis for performance-based design for pile-founded flexible approach walls.

At the time of publication, COL Bryan S. Green was the Commander, ERDC, and Dr. Jeffery P. Holland was Director.

Unit Conversion Factors

Multiply	By	To Obtain
cubic feet	0.02831685	cubic meters
cubic inches	1.6387064 E-05	cubic meters
cubic yards	0.7645549	cubic meters
degrees (angle)	0.01745329	radians
feet	0.3048	meters
foot-pounds force	1.355818	joules
horsepower (550 foot-pounds force per second)	745.6999	watts
inches	0.0254	meters
inch-pounds (force)	0.1129848	newton meters
knots	0.5144444	meters per second
microinches	0.0254	micrometers
microns	1.0 E-06	meters
miles (nautical)	1,852	meters
miles (U.S. statute)	1,609.347	meters
miles per hour	0.44704	meters per second
mils	0.0254	millimeters
pounds (force)	1000.0	kips
pounds (force)	4.448222	newtons
pounds (force) per foot	14.59390	newtons per meter
pounds (force) per inch	175.1268	newtons per meter
pounds (force) per square foot	47.88026	pascals
pounds (force) per square inch	6.894757	kilopascals

1 Introduction

More than 50% of the U.S. Army Corps of Engineers' (USACE) locks and their approach walls have continued past their economic lifetimes. As these structures wear out they must be retrofitted, replaced, or upgraded with a lock extension. Innovative designs must be considered for these Corps hydraulic structures, particularly flexible approach walls, and new tools for evaluating these designs must be developed.

Guide and guard walls are structural features that barge trains use to align with and enter the lock chamber. These approach walls are usually in the upper and lower lock approaches. Typically, a guard wall is located on the streamside of the lock, i.e., the wall in extension of the lock wall nearest to the dam.[1] A guide wall is strictly an alignment mechanism that does not protect the barge train from river currents (Park 2002). A guide wall is an extension of the wall of the lock that is typically located nearest and generally parallel to the bank. Both guard and guide walls may be referred to as lock approach walls.

Pile-founded, energy-absorbing, flexible-lock approach walls are being adopted by the Corps because they are cost-efficient, yet can withstand barge train impacts. They are used for upstream and downstream guide and guard walls. Because most pile-founded approach wall structures can take advantage of in-the-wet construction techniques, where a site does not have to have a cofferdam and be dewatered for construction, a substantial cost savings is achieved. Because these structures are based on piles that flex, the energy of a barge train impact is absorbed in the flexible capacity of the system. A further reduction in the construction costs of these structures, while maintaining capacity, can be achieved by a systematic approach for minimizing the length of the piles placed, which would reduce the pile material costs and amount of effort to place these piles. A reduction in the length of the supporting piles, while maintaining the overall capacity, will result in cost-efficiency gains.

[1] A guard wall protects the barge train from danger of being carried over the dam in high water. It acts to enhance the safety of navigation as well as the safety of locks themselves.

1.1 Examples of flexible, pile-founded approach walls

Figures 1.1 through 1.6 show the design and scale of these projects. Though these images are specific to drilled-in-pile (DIP) founded bents supporting an impact-beam, the scale and consideration involved also apply to impact decks supported on piles. Notice that the Marmet pile bent in Figure 1.1 shows that the bent will have a load applied at approximately 26-29 ft (312-348 in.) above the mudline, and a 38 ft (456 in.) depth of embedment. Figure 1.2 shows bents for an approach wall at Marmet Lock and Dam before impact beams have been placed. Figure 1.3 shows beam sections being transported to Marmet Lock and Dam. Figure 1.4 shows the beam being placed after the site has been flooded and Figures 1.5 and 1.6 show a similar situation at Winfield Lock and Dam.

Figures 1.7 through 1.9 show the plans and installation of an impact deck approach wall extension constructed at Lock and Dam 3. Lock and Dam 3 is located on Mississippi River mile 796.9 near Red Wing, MN in St. Paul District. The impact deck is monolithic in nature and supported by multiple rows of pile groups, as shown in Figure 1.8. Dynamic structural response analyses using Impact_Deck software have shown that there is significant load sharing among multiple rows of clustered pile groups with a monolithic impact deck[1]. Load sharing among the rows of piles reduces the portion of design impact load per row. Lower design loads translate into smaller cross-section and/or fewer piles. The Lock and Dam 3 approach wall extension used a batter pile configuration with 2-foot diameter pipe piles filled with concrete. This configuration could have also used cast-in-drilled-hole (CIDH) reinforced concrete (RC) piles. For the less costly in-the-wet construction, RC piles are drilled in place and the base of the deck can be pre-formed and attached to the piles as they were for Lock and Dam 3. The rest of the deck can then be formed and poured on-site.

This report will focus on vertical pile systems. Ebeling et al. (2012 and 2013) have shown that vertical pile configurations often allow greater deformation and have more flexibility than batter pile systems. Deformation-based design procedures for batter-pile systems are the subject of the next phase of research.

---

[1] White, B. C., J. R. Arroyo, and R. M. Ebeling. 2015. *Simplified dynamic structural time-history response analysis of flexible approach walls founded on clustered pile groups using Impact_Deck*. In *Preparation*, ERDC/ITL TR-16-X. Vicksburg, MS: U.S. Army Engineer Research and Development Center.

Figure 1.1. Plans for the Marmet structural impact beam with two DIPs.

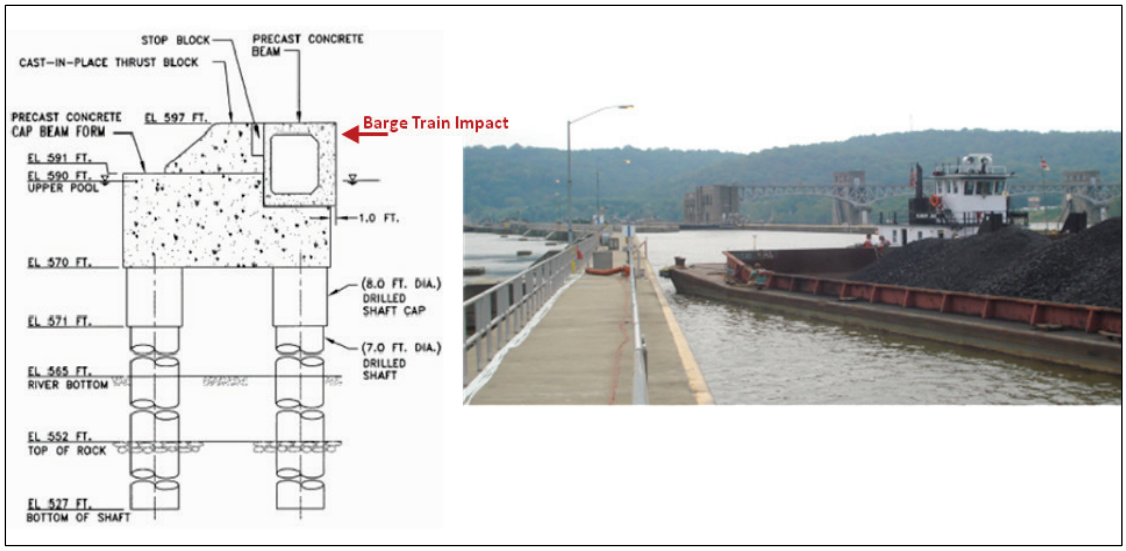

Figure 1.2. A set of two-DIP bents at Marmet approach wall to be used to support impact beam sections.

Figure 1.3. Marmet approach wall impact beam sections on barge for transport.

Figure 1.4. Installation of the Marmet approach wall impact beam sections.

Figure 1.5. Installation of impact beam sections for the Winfield Lock and Dam approach walls.

Figure 1.6. Another view of the impact beams used for the approach wall for Winfield Lock and Dam.

Figure 1.7. Plans for an impact deck structure at Lock and Dam 3.

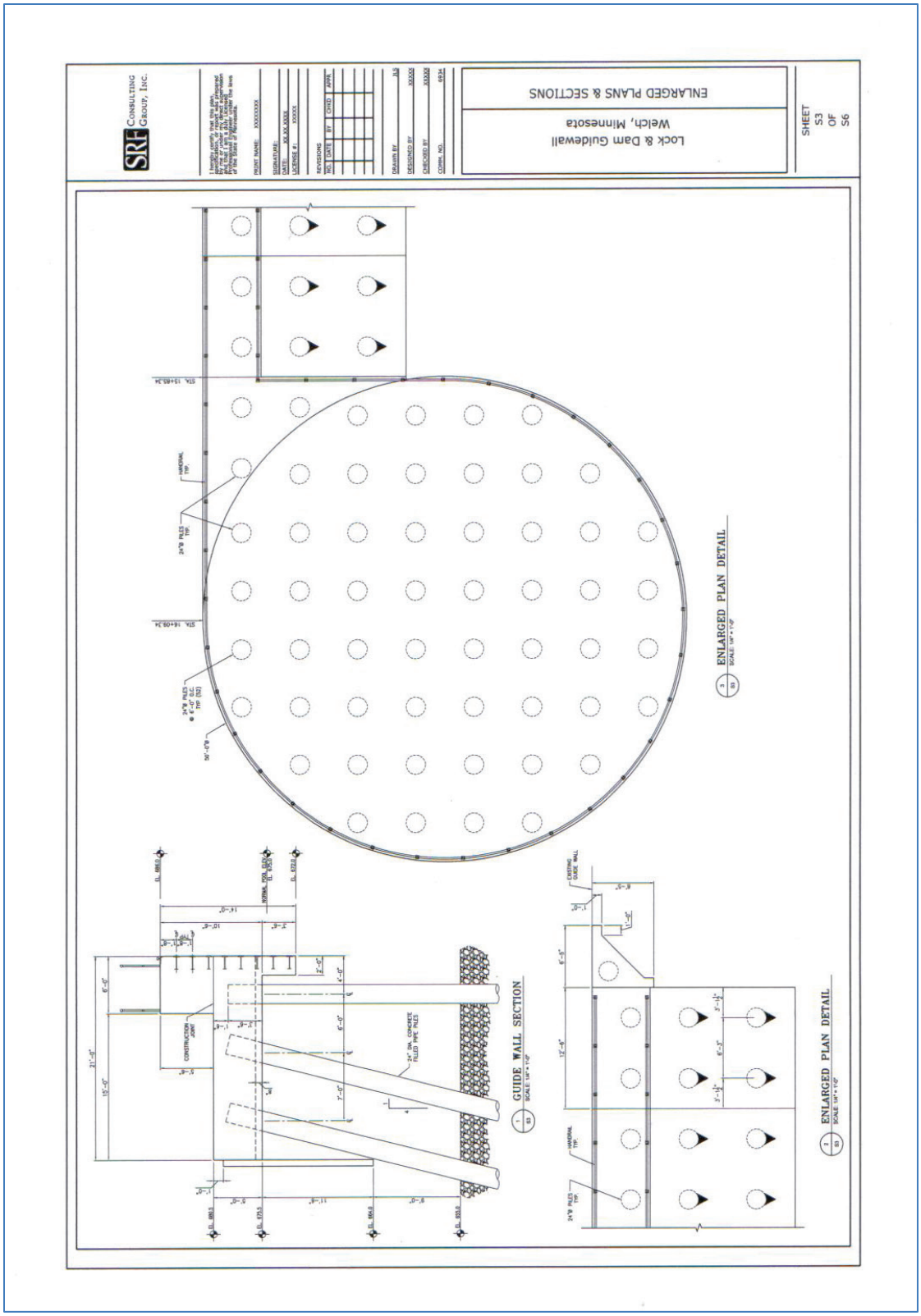

Figure 1.8. In-the-wet construction for the impact deck at Lock and Dam 3.

Figure 1.9. The finished pile-founded impact deck approach wall at Lock and Dam 3.

1.2 Construction techniques for flexible, pile-founded approach walls

Pile-founded flexible lock approach walls are typically constructed with impact beams simply supported on pile bents or by using an impact deck supported by groups of clustered piles. CIDH RC piles have seen recent widespread use as a cost-effective method of transferring superstructure loads into the soil or rock foundation, given sufficient depth of embedment. The primary design load for lock approach walls are dynamic barge train impacts on a beam or deck. The primary loading is transverse to the line of the approach wall. These bents and decks are supported tens of feet above the mudline and barge impacts occur at the beam or deck level (i.e., lateral loading at the top of the pile). Because of this lateral loading at the pile cap, vertical pile groups must be designed to exhibit long-pile behavior as defined below.

Short-pile behavior is associated with a relatively short, stiff pile subjected to sufficient lateral shear and overturning moment, for which the lateral resistance of the soil is mobilized along the entire length of the pile (Broms 1965; Brown et al. 2010). A key observation is that the short, stiff pile tends to rotate as a rigid body (e.g., Figure 1 in Broms 1965). Long-pile behavior is defined as the behavior that an embedded pile exhibits when its pile cap deflection under a lateral load at the pile cap does not vary significantly from a pile with an extreme embedment.

For piles exhibiting this long-pile behavior, design loads introduce substantial moments for the vertical piles at a short distance below the mudline. Methods for estimating the minimal vertical-pile tip depth of embedment that gives long-pile behavior are investigated and improvements are suggested. Reducing the length of piles will result in a cost savings for Corps projects, especially for in-the-wet construction.

1.3 Investigation of mudline hinge depth by Janoyan, Wallace, and Stewart

Janoyan et al. (2001) conducted a full-scale, test-to-failure of an instrumented CIDH shaft/column founded in stiff clay to investigate derived p-y curves for their 6-ft-diameter pile. Structural details implemented for application of loading to the top of this shaft/column resulted in a pinned head top of pile boundary condition. Other details regarding the interpretation of these test results are also discussed in

Janoyan et al. (2006). The CIDH shaft details for this test specimen were a diameter of 6 ft, and a length of 88 ft (1056 in.), with the shaft extending 48 ft (576 in.) below ground and 40 ft (480 in.) above. The CIDH shaft was designed according to the California Department of Transportation (CDOT) standards using *Caltrans Seismic Design Criteria* (CDOT 1999). These specifications roughly correspond to the example problem used for this report, discussed in Chapter 2.

The single CIDH shaft/column was able to sustain a lateral load of approximately 315 kips. Yielding of the reinforcement occurred between 12 and 24 in. displacement cycles. However, a significant reduction in load capacity was not observed until shaft displacements reached approximately 9 ft (108 in.). Loss of capacity occurred due to fracture of the longitudinal reinforcement bars approximately 5 ft below ground line (approximately 0.8 times CIDH diameter).

From the Janoyan article, especially Figure 6 of the article, the relationship between moment and curvature field inferred at the ground line (called the mudline in our analyses) was greater than the moment-curvature derived by an analytical method. The maximum moment from the field inferred at the ground line (mudline) is approximately 145,000 kip-in., while the maximum moment computed at the mudline by a traditional section analytical model is approximately 130,000 kip-in. Both curves are asymptotic to their peak moment values after a curvature of 0.0001 (1/10,000 in.) develops in the CIDH test shaft/column.

During this investigation, the authors of this report studied the curve-based data contained in the Janoyan et al. (2001) Figure 7 for test shaft slope and deflected shape distributions given the 6 in. displacement level stage in their field test. It was observed that the shaft slope drops off dramatically at 18 ft below ground surface. This depth corresponds to approximately 3 times the CIDH diameter. Contrasting the two curves, a constant shaft slope forms below 18 ft depth and displacement diminishes with depth, at a constant rate until it reaches zero at a pile tip of 48 ft.

1.4 Introduction to performance-based design methodology for calculating pile embedment for use in the Corps' Flexible Approach Walls

In bridge design, it is common practice to use an allowable stress (service) load design approach or an ultimate strength (factored) load design

approach. The service load is established based on predicted long-term conditions and the factored load is a conservative scaling of the service load for unpredictable events.

The Corps, however, is proposing a performance-based design approach for lock approach walls subject to barge impact with a serviceability performance objective for usual barge impact loads, a damage-control performance objective for unusual barge impact loads, and a collapse-prevention performance objective for extreme barge impact loads (HQUSACE 2004).

Headquarters, U.S. Army Corps of Engineers (HQUSACE 2005) specifies three design-load events for a structural system based on probability of occurrence. Table 1.1 provides the list of load condition categories (Usual, Unusual, and Extreme), annual probabilities of these events, the return period of these events, and the performance objective of the structure during these events (HQUSACE 2004). These probabilistic events can be used to determine, for a given barge train, an appropriate approach velocity and angle for an impact.

Table 1.1. Design load events according to HQUSACE 2004 and 2005.

Load Condition Category	Annual Probability (p)	Return Period (t_r)	Performance Objective
Usual	p>=0.10	t_r <=10 yrs	Undamaged barge approach wall
Unusual	0.10>p>=0.0033	300 yrs >=t_r >10 yrs	Minor, repairable damage
Extreme	P<0.0033	t_r >300 yrs	Moderate to extreme damage without complete collapse of structure

Satisfying the collapse prevention objective in the Extreme event generally assures that the other two performance objectives will be met. Flexural plastic hinging is permitted in DIP under extreme load conditions. Recent ERDC research (Ebeling et al. 2012) has developed simplified analysis procedures for flexible approach wall systems founded on clustered groups of vertical and batter piles subjected to barge train impact. The procedure described in this 2012 report is referred to as “pushover” analysis of a single clustered pile group. This procedure quantifies the deformation-related, potential energy-absorption capacity of the flexible structure before structural collapse. Therefore, pile-embedment depth methods that provide adequate long-pile behavior for maximum lateral-load capacity as determined by collapse mechanism (pushover) analysis result in a flexible impact structure that deforms to absorb energy, but has the minimum pile-

cap deformation before pushover in an extreme event. Having flexible approach wall structures with minimal deflection under extreme impact events is a desirable design attribute.

In the design process, the pushover analysis can be performed using excessively long piles in the model ensuring long-pile behavior in order to determine if the structural capacity meets the Extreme load condition specified in HQUSACE (2004 and 2005). At this stage, design changes affecting the cluster pile-group capacity can be made by altering the pile cap, the number of piles, and/or the moment capacity of individual piles until the design ultimate capacity satisfies the performance objective for the Extreme impact event. This design process attempts to minimize the cost of the structure while still meeting the performance objectives. Following this line of thought, one approach is to set the impact design load value for the Extreme event to the desired maximum lateral load capacity of the clustered pile group. This capacity is the sum of the capacities of each pile within the pile group before the first hinging action of any pile. If the capacities of all the piles are the same, then the capacity of an individual pile is equal to the Extreme event load divided by the number of piles. For the required pile capacity, the design process and capacity analysis are iterated to find the pile properties (i.e., reinforced concrete pile diameter, amount of reinforcing steel, etc.). General design guidance for pile foundations is provided in HQUSACE (1991).

Barge train collisions with an approach wall are routine impact events that occur as the barge train attempts to align itself for entrance into the lock. Impact events are rarely static in nature. They have dynamic force-time histories (Ebeling et al. 2010) and travel along the impact beam or deck. Recent research[1] has shown that the geometry and material properties of the flexible structural features can amplify the peak forces occurring at a clustered pile group due to interacting frequency response for impact beam structural systems and the dynamic impact event. This research also shows that peak loads of the dynamic response can be distributed among neighbor clustered pile groups for impact deck structural features, reducing the peak force any clustered pile group may encounter. Because

[1] White, B. C., J. R. Arroyo, and R. M. Ebeling. 2016. *Simplified dynamic structural time-history response analysis of flexible approach walls founded on clustered pile groups using Impact_Deck*. In *Preparation*, ERDC/ITL TR-16-X. Vicksburg, MS: U.S. Army Engineer Research and Development Center.

the impact event load amplification and/or distribution is dependent on the geometry and material properties of the structural system, any design changes (e.g., changing the number of piles in the clustered group, changing the pile moment capacity, changing the pile cap, etc.) must be reassessed to determine the peak load during an Extreme impact event in an incremental design process.

Strength design methods, per the American Concrete Institute (ACI), are used to establish drilled-in-pile capacities. Since soil-structure interaction methods are used to establish load-displacement characteristics in this method, a characterization of pile cracked-section stiffness (EI) is accounted for in the analysis.

When the design satisfies the performance objective for the Extreme impact event, then the pile depth of embedment can be adjusted to a minimal depth that guarantees long-pile behavior. This process is independent of the iterative design procedure, and only needs to consider the final design and the final pushover analysis capacity.

1.5 Using pushover analysis in a performance-based design

In order to meet the fundamental objective of the design, the designer must determine the minimum depth-of-embedment for a vertical pile so that it may resist lateral loading up to the ultimate load as defined by the hinging actions of a pushover analysis and satisfy long-pile behavior.

Several "state-of-practice" methods exist in the pile design literature for the estimation of pile embedment to guarantee long-pile behavior. Because these state-of-practice methods come primarily from the bridge industry, these pile-embedment depth methods are based on factored and service loads.

Ebeling et al. (2012) proposes a performance-based design procedure that would use a pushover analysis in the design of pile-founded approach walls. The pushover analysis described in Ebeling et al. (2012) is an incremental analysis to determine the energy-absorption capacity of the pile-founded structure. The energy that must be absorbed is for barge train impacts with different load condition categories of Usual, Unusual, and Extreme, given their probability of occurrence (Table 1.1). The kinetic energy imparted by the barge train normal to the pile-founded approach

wall is a function of its mass (m), velocity (v), and angle of impact to the approach wall from the line parallel to the wall (θ), which are all based on the load condition category. The kinetic energy (KE) is given by:

$$KE_{BargeTrain} = \frac{m(v * \sin\theta)^2}{2} \quad (1.1)$$

The pile-founded approach wall absorbs this energy by deformation of the piles in a spring reaction. However, as the structure absorbs energy, each of the piles deform until excessive moments cause flexural yielding, allowing hinging of the structure. This flexural yielding reduces the capacity of the structure, and will eventually lead to the structure being "pushed over."

The pushover analysis determines the potential energy capacity of the structure until the structure can provide no more resistance to the impact event.

Figure 1.1 shows a typical plan for an approach wall that is based on a simply-supported impact beam placed on a vertical pile-founded, concrete bent. In this case, the two piles have similar cross-section properties and each pile is assumed to share nearly half the weight of the bent and beam. Another example of this type of structure is analyzed in Chapter 2 of this report. For that example, the piles are embedded in a homogeneous soil. The piles are assumed to be fixed against rotation where the pile top meets the bent. Given this configuration, the piles will deform nearly synchronously with each pile bearing nearly half the load that occurs normally to the approach wall.

The example in Chapter 2 contains two points on each pile where the moments will rise until yielding occurs. These hinge points are at the point of fixity, where the top of pile meets the bent, and at a short distance below the mudline where the soil restrains the pile.[1] For the hinge point where the pile cap meets the bent, hinging means that while the pile is still connected to the bent, there is no moment transfer from the bent to the pile cap. While this condition is undesirable and will need to be repaired, the approach wall will still have energy-absorbing capacity. If hinging

[1] Janoyan et al. (2001), with a 40 ft exposed length, 6-ft-diameter CIDH pile similar to the example problem of Chapter 2 (except for clay soils and pinned pile head) found this hinge point to occur 5 ft below the mudline, or 0.8 times the pile diameter.

occurs at the second possible hinge point a short distance below the mudline, then that the structure is unrepairable (due to its location of below water and below the mudline) and near collapse, with little residual capacity to absorb additional barge train impact energy.

For the pushover analysis, the moment capacity at these two possible hinge points is evaluated based on the material properties of the pile, the confinement pressure due to the weight of the beam, and the additional weight of the pile above the hinge point a short distance below the mudline. In general, for uniform piles, the pile-cap hinge point has less moment capacity than the mudline hinge point. For the 40 ft exposed pile example, the moment capacity at the pile cap was 143,880 kip-in. and the capacity at the mudline was 146,640 kip-in.

For the first incremental load step, the lateral load at the pile cap is given an arbitrary value and the possible hinge points are monitored to determine if the moment at that hinge point exceeds the hinge-point capacity. Because the change in moment is linear with respect to the load force for this portion of the curve, a second iteration is all that is necessary to determine the peak force to the first hinge point, interpolating through the origin. For the example problem introduced in Chapter 2, pile-cap hinging occurs before mudline hinging, when the lateral pile-cap load is 367 kips and the pile-cap deflection is 12.1 in. This is shown as the first inflection point in Figure 1.10.

The second incremental load step continues the process, but because of the hinging at the pile cap, the fixity at the pile cap is released with respect to rotation, so that the pile cap is pinned. At the beginning of this incremental load step, the lateral force imposed at the pile cap is 367 kips, but a significant resultant moment (-143,880 kip-in.) is introduced at the pile cap when the pile goes from a fixed boundary condition to a pinned boundary condition. Starting with this load case, the lateral load is set to a higher value than the first hinge load. Because the change in moment is linear with respect to the load force for this portion of the curve, a second iteration is all that is necessary to determine the peak force to the first hinge point, interpolating through the first hinge point. The change in lateral load was 81 kips, resulting in a final lateral load of 448 kips in total. The deflection at this point was 28.9 in. This is shown as the first inflection point in Figure 1.10.

Figure 1.10. Pushover curve for a single vertical pile in the example problem.

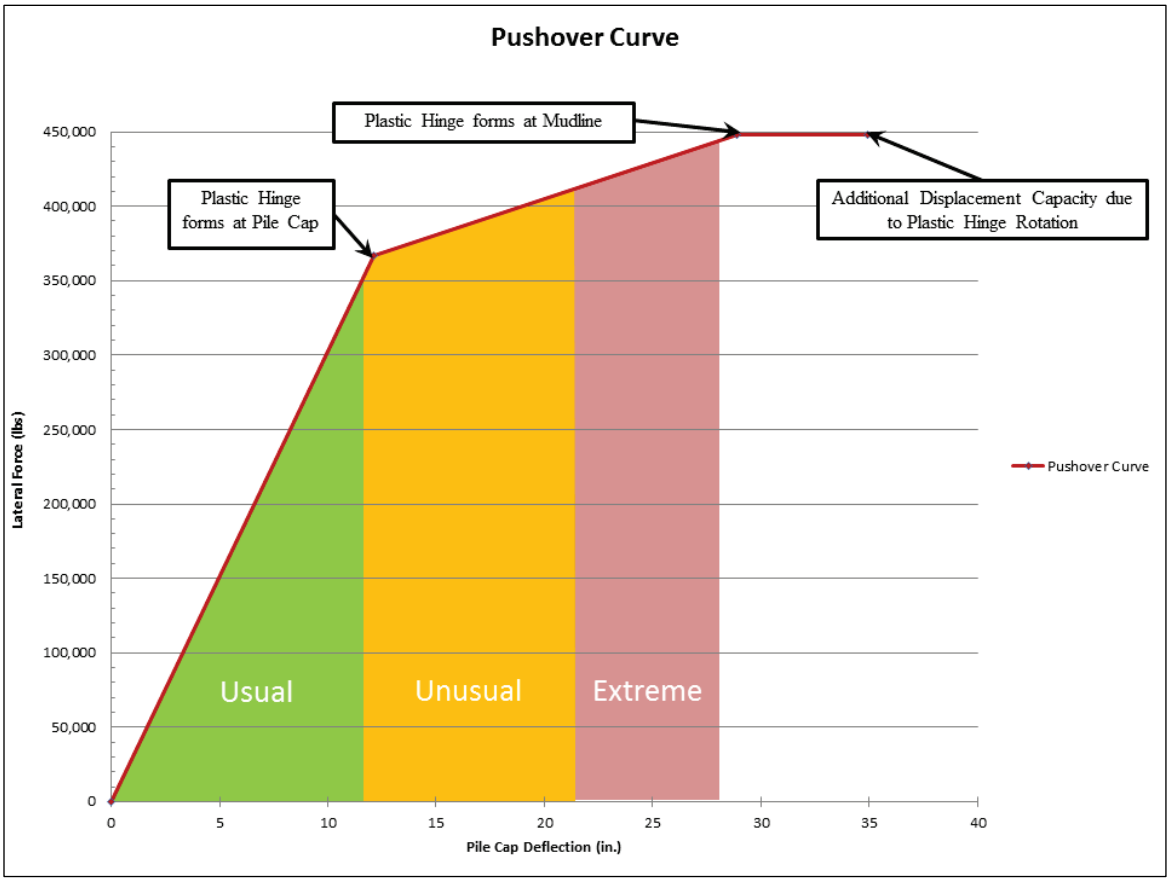

The additional displacement capacity is determined according to the process in Appendix A, section A.10 of Ebeling et al. (2012). The amount of energy that the system is capable of absorbing is revealed by the area of the colored regions for the Usual, Unusual, and Extreme load cases. The energy that can be absorbed in the Usual condition is covered by the green area. Since this region terminates to the left of the first plastic hinge, it satisfies the required serviceability performance criterion. For the Unusual condition, the energy that can be absorbed is covered by the green and yellow area. Since the extent of this region lay to the right of the first plastic hinge formation at the pile cap, but before hinging below the mudline, a reparability criterion would be satisfied when this Unusual load case is achieved. Finally, for the Extreme condition, the energy that can be absorbed is covered by the green, yellow, and red areas. In order to satisfy the non-collapse performance requirement and provide a margin of reserve energy capacity for collapse prevention, this zone should terminate before the plastic hinge formation below the mudline.

The ERDC research effort summarized in this report examines these methods with respect to a pushover analysis of a vertical pile-founded

structure in an effort to determine which methods are conservative or liberal in their assessment of pile embedment to assure long-pile behavior. By assessing the results of the different state-of-practice methods for assigning length to assure long-pile behavior, a systematic approach to guarantee long-pile behavior is determined using the pushover capacity for a long-pile system.

1.6 Report contents

Chapter 2 investigates the state-of-practice methods in existence for estimating the pile tip depth of embedment guaranteeing long-pile behavior. An example pile-founded approach wall structure design is introduced. A pushover analysis is described for this structure, with attention placed on the effects of the cohesionless soil. The pushover analysis determines the peak force applied at the pile cap before pile hinging at a short distance below the mudline occurs. This peak force is applied to the pile for subsequent discussions of the methods for determining the pile depth of embedment for long-pile behavior in the example problem. Values for pile depth of embedment are evaluated by analyzing the pile using the existing methods. Observations gleaned from these analyses led the authors of this report to the development of another method based on the difference of pile-tip deflection over the change in pile tip depth of embedment. The resulting pile tip depths of embedment for the previously existing methods and the new method are compared. To verify the validity of the new procedure, a pushover analysis and the systematic inflection point in the pile-tip deflection versus pile tip depth of embedment asymptotic curve analysis are performed on a pile with a different exposed height and the results are discussed.

Chapter 3 summarizes the discussions in Chapter 1 and Chapter 2, restating the reasons for this investigation and the iterative nature of design before the pile depth of embedment can be determined. The reasoning and conclusions of Chapter 2 are revisited, with attention focused on the variable nature of the pile systems, leading to the conclusions that a systematic system is better than a state-of-practice solution.

Appendix A discusses the effects of using “smeared crack” pile properties (and thus, the advisability of using COM624G for analysis) for the incremental pushover design method, as compared models that start with uncracked properties for the pile and add cracked sections to the pile as

the load is increased (e.g., LPILE). A pushover analysis is performed to the first increment, and the calculated force, deflections, and moments are compared between the models.

2 Methods to Determine Vertical Pile Depth of Embedment for Long-Pile Behavior

2.1 Introduction to pile-depth methods

Ebeling et al. (2012) reviewed thirteen methods for determining minimum safe depth of embedment for piles exhibiting long-pile behavior. For these methods, long-pile behavior is assumed to be the behavior under an applied lateral load where the pile has negligible change of deflections, shears, and moments below some point along its length according to Figure 2 of the Davisson (1970) report. Recall that the definition of long pile behavior in this report is only based on pile cap deflection. The Davisson criteria will meet the defined pile cap deflection criteria, but may result in excessive pile-tip embedment depths. Of these thirteen methods, six methods warranted further review: the Davisson (1970) method; three methods reviewed in Lien (2011); a method by Reese et al. (1970); and a procedure based on the work of Budek et al. (2000), using a prescribed limit for the asymptotic approach reviewed by Lien in 2011.

The Davisson (1970) method is based on the "stiffness" of the pile, given by the relative stiffness factor equations. For clay soils and rock the equation is

$$R = \sqrt[4]{EI / E_s} \tag{2.1}$$

where R is the relative stiffness factor, EI is the bending stiffness of the pile, and, E_s (in units of force/length^2) is the horizontal subgrade modulus, independent of embedment depth. For sand sites, which we will be examining, the equation is

$$T = \sqrt[5]{EI / n_h} \tag{2.2}$$

where T is the relative stiffness factor, n_h is the soil stiffness, and where $E_s = n_h x$ stiffness increases from the top of the mudline to the tip of the pile (and indirectly, with the confining pressure). According to Davisson

(1970), the depth of embedment (D) for long-pile behavior could be determined by using the equations

$$D = 4R \text{ , and} \tag{2.3}$$

$$D = 4T \tag{2.4}$$

for clay or sandy soils, respectively.

The three methods discussed by Lien (2011) depend upon the curves of horizontal deflection versus depth of embedment. In order to compute the deflections, loads must be applied to the pile models. While the loads typically used for these calculations are the "factored" and "service" loads, the load applied in this report is the ultimate capacity force developed under a pushover analysis. Recall that the factored load for a single pile is determined from an Extreme event load applied to a clustered pile group as discussed in section 1.3. The moment capacity of the pile within the region of the mudline is used to back-calculate the factored load value with consideration to the moment arm. The force applied at the pile cap to induce this moment in the pile is determined using a pushover analysis described in Ebeling et al. (2012) and discussed below.

2.2 Pushover analysis of a flexible approach wall founded on a pair of 40 ft exposed vertical piles

For the pushover analysis of a single elevated pile group (Figure 2.1), we assume that each pile possesses a fixed-head boundary condition[1] at the pile-to-pile cap interface until the moment capacity of the drilled-in-place pile is exceeded at the pile-to-pile cap interface, resulting in a hinging action occurring at this location and the loss-of-fixity at this point for the two vertical piles. From this point, the pushover analysis can linearly interpolate the horizontal loading that is required with a pinned-head, pile-to-pile cap connection, with the final fixed head moment at the pile

[1] General guidance is provided by Castella et al. (1984) for vertical H-Pile embedment length to obtain pile-to-pile cap fixity. When H-Pile embedment is more than twice the pile depth or diameter, the rotation of the pile reaches a minimum constant value independent of embedment length which indicates that the fixed-head condition is achieved. Recent ERDC 3D finite element analyses of pile-to-pile cap embedment behavior have been performed for a HP14 x 89 pile embedded for a length of 16.77 in. along the neutral axis. For this pile-to-pile cap embedment, the moment capacity at the pile cap is about 80% of the moment capacity for a fixed head condition (Ebeling et al. 2014). This general information suggests that pile head fixity can be assumed given sufficient pile-to-pile cap embedment. Fixity may also be achieved through structural detailing of the pile (e.g., DIP, etc.) and the pile cap.

cap, until the moment capacity within the drilled-in-place pile is exceeded. This typically occurs within the vertical pile region located just below the mudline and results in a second hinging of the pile at a short distance below the mudline. A structural mechanism starts to form for the elevated pile system when the two piles hinge a short distance below the mudline.

Figure 2.1. An example of a typical two-pile bent structure.

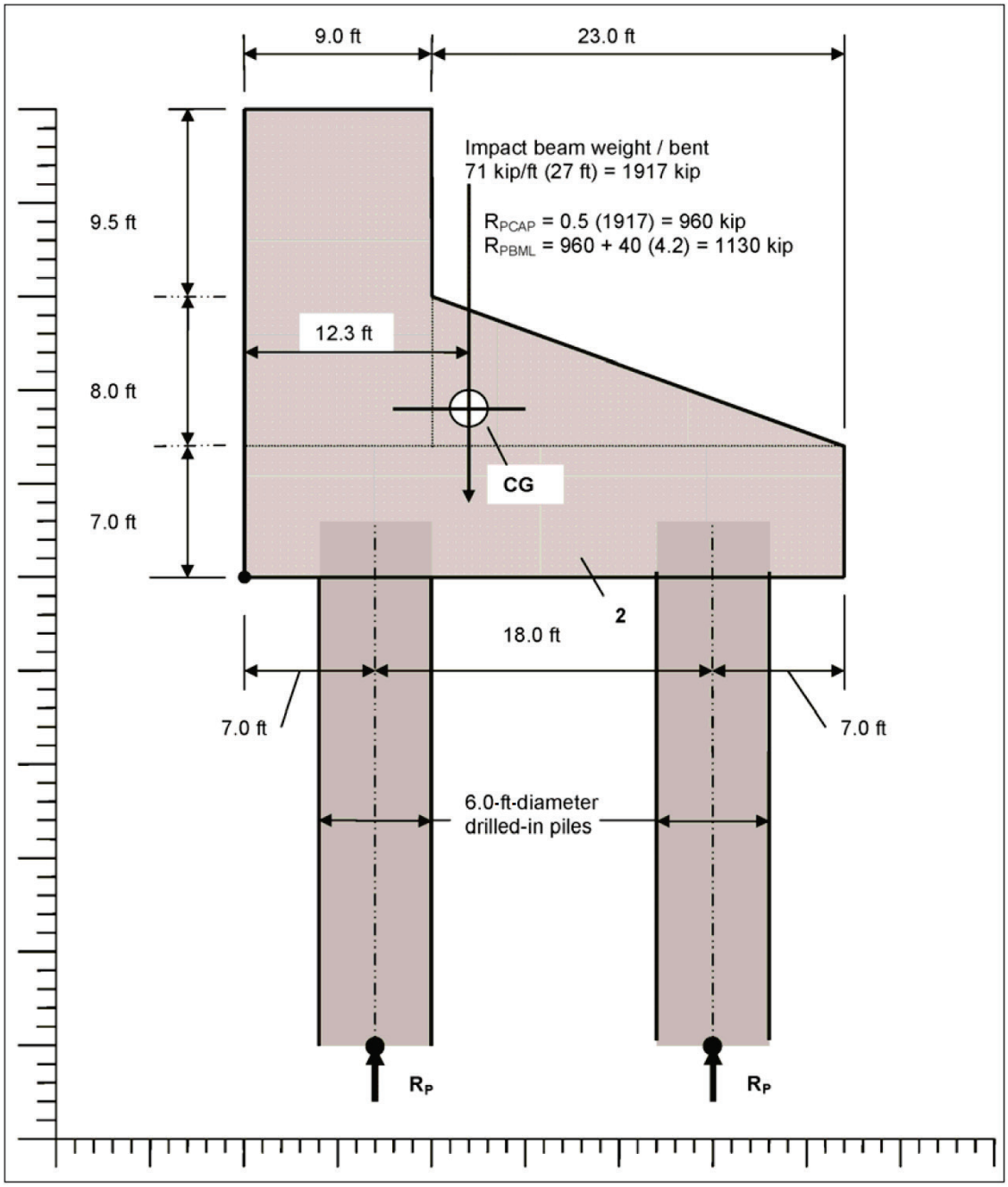

For the Ebeling et al. (2012) pushover analysis examples being considered, a pair of vertical, 6-ft-diameter, circular drilled-in-place piles is considered. The model pile is assumed to be 100 ft long for the initial analyses, with 40 ft above the mudline and 60 ft below the mudline for the pushover analysis. The caisson section has 18 bundled #14 rebar sections (Figure 2.2). These rebar sections are placed at 20 degree intervals 6 in. from the outside of the pile. The properties of the materials are presented in Table 2.1.

Figure 2.2. An example cross-section of a 6 ft diameter, circular drilled pile with rebar.

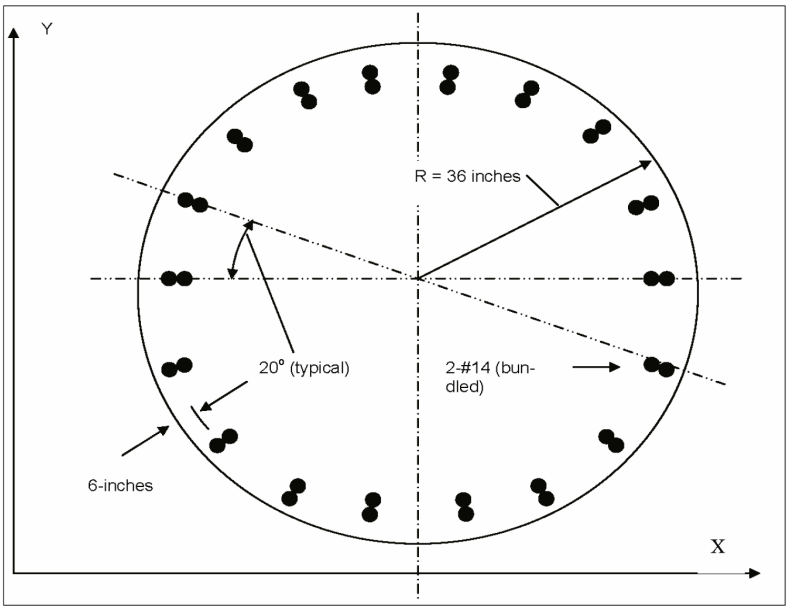

Table 2.1. Input parameters for the example 2-pile bent with 6-ft-diameter, circular drilled-in-place piles (DIP).

Area of DIP	A_p	28.274 ft^2
Moment of inertia of DIP	I_p	63.617 ft^4
Effective moment of inertia of DIP	I_e	15.90 ft^4
Yield strength of steel	f_y	60.0 ksi
Steel modulus	E_{steel}	29,000.0 ksi
Strain stress hardening	ε_p	0.01
Usable strain to prevent fracture of rebar	$\varepsilon_{s\text{-}ult}$	0.05
Ultimate stress at fracture	f_u	60.01 ksi
Concrete compressive strength	f'_c	4.0 ksi
Concrete modulus	$E_{concrete}$	3,500.0 ksi
Ultimate strain	$\varepsilon_{c\text{-}ult}$	0.003

In this example, several assumptions are being made regarding the values assigned to the Table 2.1 material properties so as to keep the analysis simple and to err on the conservative side:

- These values assume an elastic-plastic behavior for the steel reinforcement with very little strain hardening for the analyses.
- Under monotonic loading, strains in the steel reinforcement up to the 15-20% range can be developed. But a 20% level of strain cannot be achieved in dynamic load reversal situations. Under a reverse-cyclic loading event which can occur during earthquake shaking, this ultimate strain value is reduced to 5% so that there are no concerns about fracturing of the longitudinal reinforcement during load cycle reversals. Barge train impact events are not anticipated to be as severe as earthquake-induced, reverse-cycle loading events, but a conservative usable strain of up to a rupture strain of 5% is assigned for this problem.
- Additionally, concrete confining pressure may be higher given the spacing and sizing of the steel hoops being used. Consequently, the ultimate strain for the confined concrete may be greater than the 0.003 value assigned in this problem.
- A smeared crack flexural stiffness is used for the entire length of the pile. This was done to satisfy the inputs for COM624G, which is the software that was used for the pushover analysis. Appendix A shows a comparison between using the smeared crack flexural stiffness approach and the discrete flexural cracked stiffness approach (e.g., an option in LPILE), where sections of the pile become cracked during a lateral load step.
- The pile bent is assumed to be a rigid member that is evenly distributed in weight over the piles. This can affect the distribution of confining pressure among the supporting piles.

The Corps' CASE library program M-PHI[1] computes the ultimate moment capacity within a single pile at both the pile cap and at the mudline. The pile-to-pile cap region of the pile is constrained against rotation as a result of the extension of the pile into the supporting bent (or impact deck) and the pouring of the concrete and placement of reinforcing steel to form the

[1] Ehsani, M. R., and M. E. Marine. 1994. *User's guide for concrete moment-curvature relationship (M-PHI)*. Tucson, AZ: MRE and Associates, U.S. Army Corps of Engineers Contract Report comes with the CASE software distribution of M-PHI.

reinforced concrete bent (or deck). Due to this constraint, the moment capacity at the cap needs to be determined because during a pushover analysis the load applied to the model may exceed the moment capacity at the pile-to-cap location, forming a hinge at the cap. Ebeling et al. (2012) observed that for these pile-founded flexible approach walls, this structural hinge will occur at this location before a second structural hinge develops within the piles at a short distance below the mudline. M-PHI calculations given in Ebeling et al. (2012) show that the piles hinge at the cap prior to hinging at the mudline. This is because of the additional confining pressure within the concrete of the piles at the mudline. The confinement within the pile concrete at the pile cap is comprised of only the weight of the bent or deck, while the confining pressure within the piles at the mudline also includes the additional weight of the pile above the mudline, increasing the pile's capacity at this lower elevation.

For this pushover calculation, a simplifying assumption is made that the axial load of the impact deck acting on the top of the pile group is shared equally between each pile. Figure 2.1 reveals that the center of gravity of the bent is between the two piles, and not exactly midway between the two piles, so this approximation is not exactly true but a close approximation. Figure 2.3 shows forces applied at the three stages of pushover. For the two-pile example, each pile supports half the weight of the impact bent/deck. The total weight of the deck is 1917 kips per vertical pile group for a pair of vertical DIP piles placed 27 ft on center, so approximately 960 kips is supported by an individual pile. For the weight acting within each pile at the mudline, the weight of the pile and impact deck above the mudline must be calculated. Each foot of pile extending above the mudline puts an additional 4.2 kips on the structure. Since in our example, the pile extends 40 ft above the mudline, the additional weight of pile is 40 ft × 4.2 kips/ft, or approximately 170 kips. Added to the weight of the bent, the weight acting on the pile at the mudline is 960 kips + 170 kips = 1130 kips.

The weight loads are shown in Figure 2.3b and Listing 2.1, where the weight acting on the pile cap is given as a force of 960 kips. For the second stage, acting at the mudline, the force acting downward is 1130 kips. This results in ultimate moment capacity of 143,880 kip-in. at the cap, and an ultimate moment capacity of 146,640 kip-in. at the mudline.

The mudline structural hinge can also withstand additional displacement based on the ultimate curvature capacity determined by M-PHI, due to the assumption that the ultimate strain capacity of the reinforcement is 5%.

From *M-PHI* analysis

$$\Phi_u = 0.0001387\ \Phi_y = 0.0000524 \text{ rads/in.}$$
$$\Phi_u - \Phi_y = 0.0000863 \text{ rads/in.}$$

Figure 2.3. How the loads are distributed among the piles and updated during a pushover analysis.

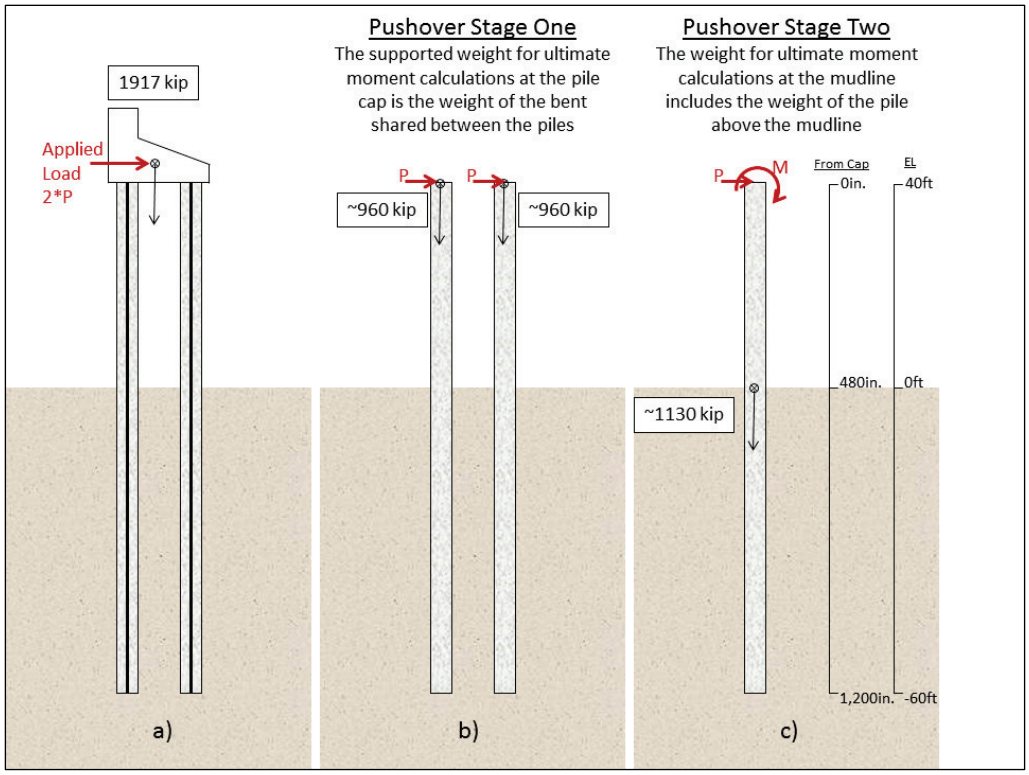

Determine plastic hinge length - L_p (per Budek et al. 2000)

$$L_p = D_p + 0.06\ L_O = 6.0 + 0.06(40) = 8.4 \text{ ft} = 100.8 \text{ in.}$$

where D_p is the diameter of drilled-in pile, and L_o is the free-standing length of the pile.

Determine plastic hinge rotational capacity – θ

$$\theta = (\Phi_u - \Phi_y)\ L_p = 0.0000863\ (100.8) = 0.0087 \text{ rads}$$

Determine additional displacement at top of pile due to plastic rotation

$$\Delta P = (\Phi_u - \Phi_y)\ L_p\ (L_O + a_T) = 0.0087\ [40 + 1.8\ (9.851) = 0.50 \text{ ft} \approx 6 \text{ in.}$$

The additional displacement capacity (ΔP) associated with the plastic hinge rotation (within the pile) provides the third and final 6 in. segment of the pushover curve, determined using M-PHI (for a single pile). Figure 4 in Janoyan et al. 2001 indicates that this may be a conservative calculation for ΔP, by their full scale test-to-failure of an instrumented CIDH 6-ft-diameter pinned-head pile with an exposed 40 ft height.

For a two-pile clustered pile-group substructure, the vertical axis force values resulting from the pushover curve would be double those force values obtained for a single pile. The x-axis displacement values do not change when altering the pushover curve results from a single pile to account for a two-vertical-pile substructure.

An ultimate moment capacity of 143,880 kip-in. (11,990 kip-ft) was computed using the M-PHI software for the example pushover analysis (Listing 2.1). This moment value corresponds to the ultimate moment capacity of the pile, with plastic hinging at the pile cap. The ultimate moment capacity of the pile at the mudline before flexural yielding occurs is 146,640 kip-in. (12,220 kip-ft), and is greater due to the confining pressure due to the additional weight of the pile above the mudline.

M-PHI determines the ultimate moment at which the pile cap forms a hinge, where the moment has a limited resistance (i.e., capacity) resisting up to that moment and no more for a fixed pile-to-pile cap connection (143,880 kip-in.). There is also an ultimate moment within the pile at a short distance below the mudline where a second hinge will form, and the pile will lose moment capacity there as well. Soil-Structure Interaction (SSI) software will be needed to determine the load that causes a moment failure and compute the subsequent deflections for the pushover analysis. CASE library software COM624G is used in this discussion.

An incremental horizontal loading procedure (Figure 2.4) is used for a pushover analysis. For the pushover analysis, start with the fixed pile-to-pile cap boundary condition. An estimate of the horizontal load required to reach the ultimate moment at the pile cap is used in a run of COM624G for a single vertical pile. With the estimated load and moment values calculated from that estimated load, a linear interpolation/extrapolation step from the origin can be used to determine the load that causes a moment in the pile approaching the ultimate moment at the pile cap. This is the first increment of horizontal load that is reported by COM624G as a load/deflection point, forming the first portion of the pushover curve.

Listing 2.1. Output for M-PHI runs for moment capacity at the pile cap and mudline for the pile, respectively.

M-PHI Input and Output for Axial Load at Top of Pile (960 k)

```
DP1 6-FOOT DIA DRILLED PILE
1
60.0 29000.0 0.01 0.05 60.01
4.0 3500.0 0.003
50 4 4
1
72.0 1.0 6.0 18 4.50 1
960.0 36.0

 MOMENT VS. CURVATURE
 (K-FT)
 CRACKING MOMENT AND CURVATURE
 MOMENT... 0.2555E+04 CURVATURE... 0.5249E-05

 YIELDING MOMENT AND CURVATURE
 MOMENT... 0.9153E+04 CURVATURE... 0.5173E-04

 ULTIMATE MOMENT AND CURVATURE
 MOMENT... 0.1199E+05 (143880 in-k) CURVATURE... 0.1420E-03
```

M-PHI Input and Output for Axial Load of Pile BML (1130 k)

```
DP1 6-FOOT DIA DRILLED PILE
1
60.0 29000.0 0.01 0.05 60.01
4.0 3500.0 0.003
50 4 4
1
72.0 1.0 6.0 18 4.50 1
1130.0 36.0

 MOMENT VS. CURVATURE
 (K-FT)

CRACKING MOMENT AND CURVATURE
 MOMENT... 0.2691E+04 CURVATURE... 0.5520E-05

YIELDING MOMENT AND CURVATURE
 MOMENT... 0.9423E+04 CURVATURE... 0.5240E-04

ULTIMATE MOMENT AND CURVATURE
 MOMENT... 0.1222E+05 (146640 in-k) CURVATURE... 0.1387E-03
```

Figure 2.4. Motion of the pile bent during pushover analysis and scale showing location of select soil p-y curves.

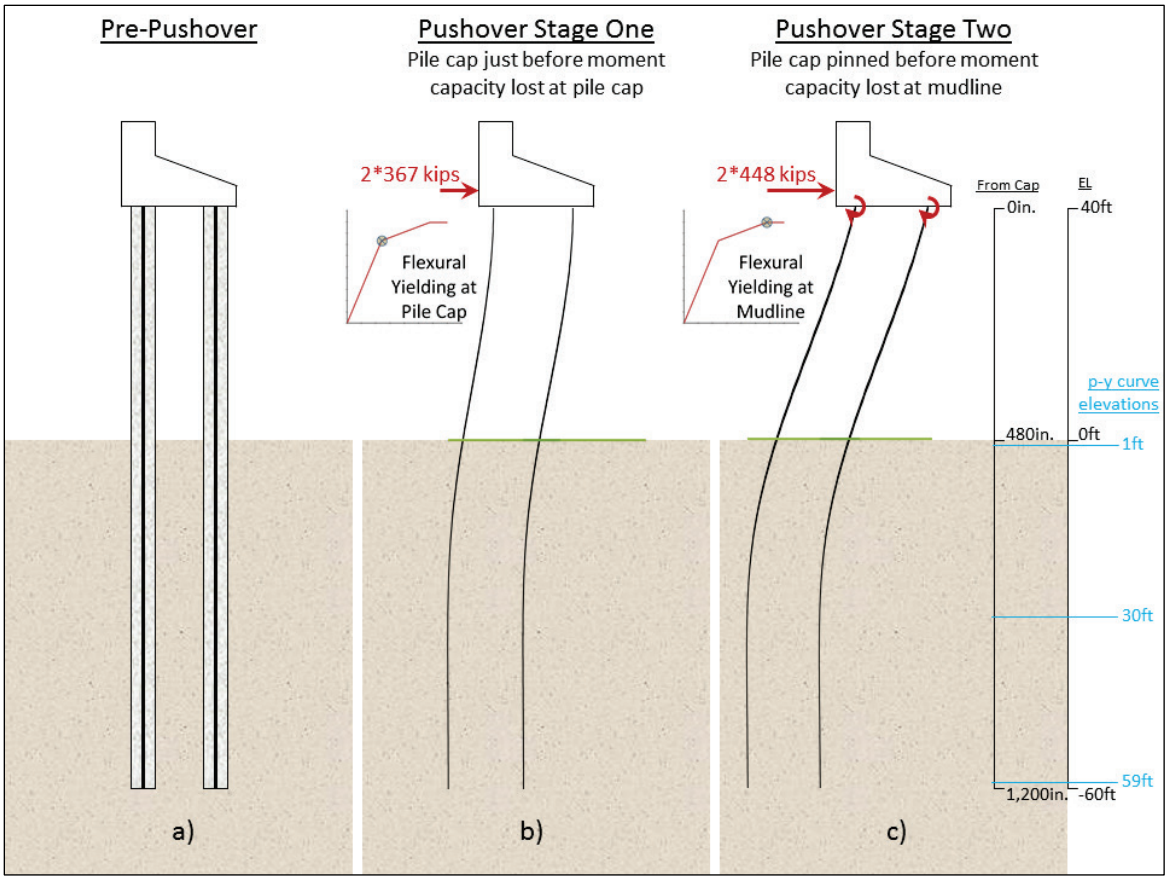

When the ultimate moment has been found at the pile-to-pile cap, the pile-cap boundary condition input for COM624G is changed to a pinned condition. This condition occurs after the loading has been applied to reach the ultimate moment at the pile cap, so the starting condition for this next increment of horizontal load includes a moment applied (as a boundary condition) at the pile cap that is equivalent to the ultimate moment at structural hinging at the pile cap. The incremental deflection of the pile cap for this second increment of horizontal load that is reported by COM624G as a load/deflection point, will be added to the first portion of the pushover curve.

For the next increment, the horizontal load at the pile cap is given an estimated value (greater than the first load), but this time the moment at a short distance below the mudline is watched to determine if the moment there exceeds the ultimate moment capacity for hinging. The load and moment pairs can be linearly interpolated/extrapolated along the line passing through the first pushover load and moment and the estimated

load and moment to determine the load when the ultimate moment at a short distance below the mudline is reached. The incremental deflection at the pile cap is captured again for the pile-to-pile cap where the load/deflection point will be added to the first part of the pushover curve. This section forms the second part of the pushover curve.

The third and final portion of the pushover curve is given by keeping the load constant and applying the additional displacement (ΔP) computed above. The computational procedure used by Ebeling et al. (2012) accounts for the additional displacement capacity associated with the plastic hinge rotation that is available with respect to flexural hinging. This load/deflection point finishes the pushover curve, as the pile has no capacity beyond that point.

COM624G provides multiple ways of specifying the soil-to-pile interactions. There are specific methods (i.e., p-y soil model curves) applied to clay and to sand soils. Specifically, there was a soil model using a criteria developed by Reese et al. (1974) for sand sites, that accommodates the increased stiffness with depth due to confining pressure that increases with depth within the soil adjacent to each pile. COM624G also allows the user to specify the soil-to-pile stiffness properties as p-y curves. For sands, a set of p-y curves must be defined, again, because the confining pressure increases with depth. In the pushover analysis performed by Ebeling et al. (2012), COM624G was performed with user-specified, p-y curves for the soil-pile interactions. For the analyses used in this discussion, the Reese sand criteria were used with the following properties: Constant K in equation $E_s = K \times x$ has a value of 30 lbs/ft^3; the effective angle of internal friction for the sand has a value of 34 degrees; and the effective (i.e., buoyant) unit weight of sand has a value of 0.0362 lbs/in.^{3} (62.6 lbs/ft^3).

Figures 2.5- 2.7 show a comparison of the p-y curves used by Ebeling et al. (2012) which are labeled as ERDC/ITL TR-12-3 (in blue) and the p-y curves calculated according to the Reese criteria in the COM624G software (in red). The bi-linear curves (in blue) were constructed using the reference deflection method as discussed in section 6.2 of Strom and Ebeling (2001) and originally proposed by Weatherby et al. (1998). The change of the p-y curves according to depth is shown for three depths in Figure 2.8. The red curve represents the soil resistance versus pile deflection of the soil at 1 ft below the mudline. The blue curve represents the soil resistance versus pile deflection of the soil at 30 ft (360 in.) below the mudline. The green curve represents the soil resistance versus pile deflection of the soil at 59 ft (708 in.) below the mudline.

Figure 2.5. Comparison of Reese sand criteria p-y curves with the p-y curves used in Ebeling et al. (2012) at 1 ft depth below the mudline.

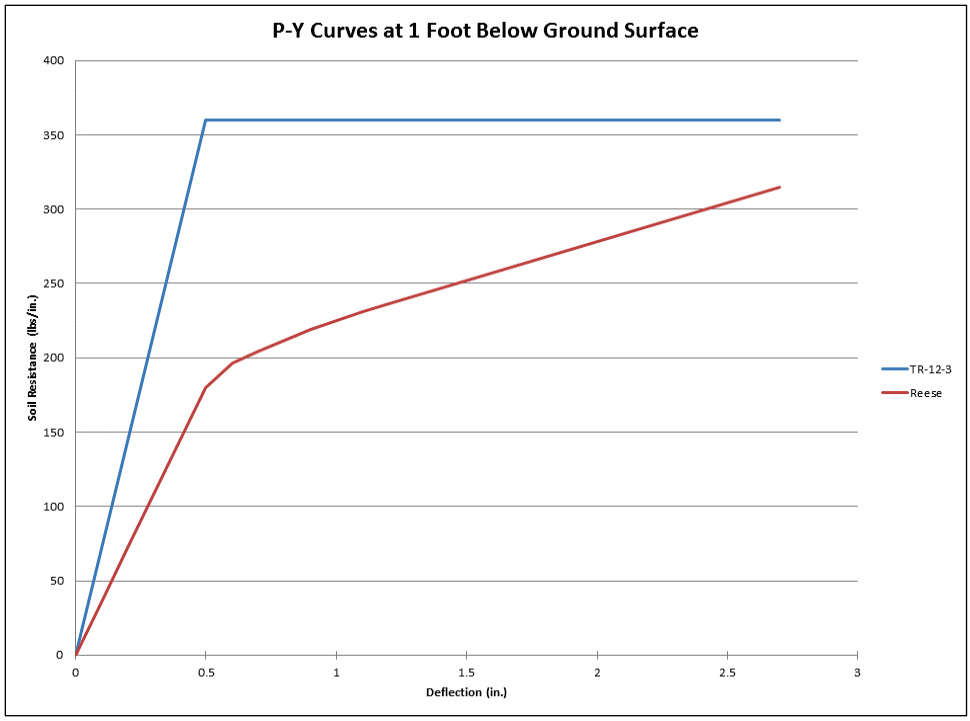

Figure 2.6. Comparison of Reese sand criteria p-y curves with the p-y curves used in Ebeling et al. (2012) at 30 ft depth below the mudline.

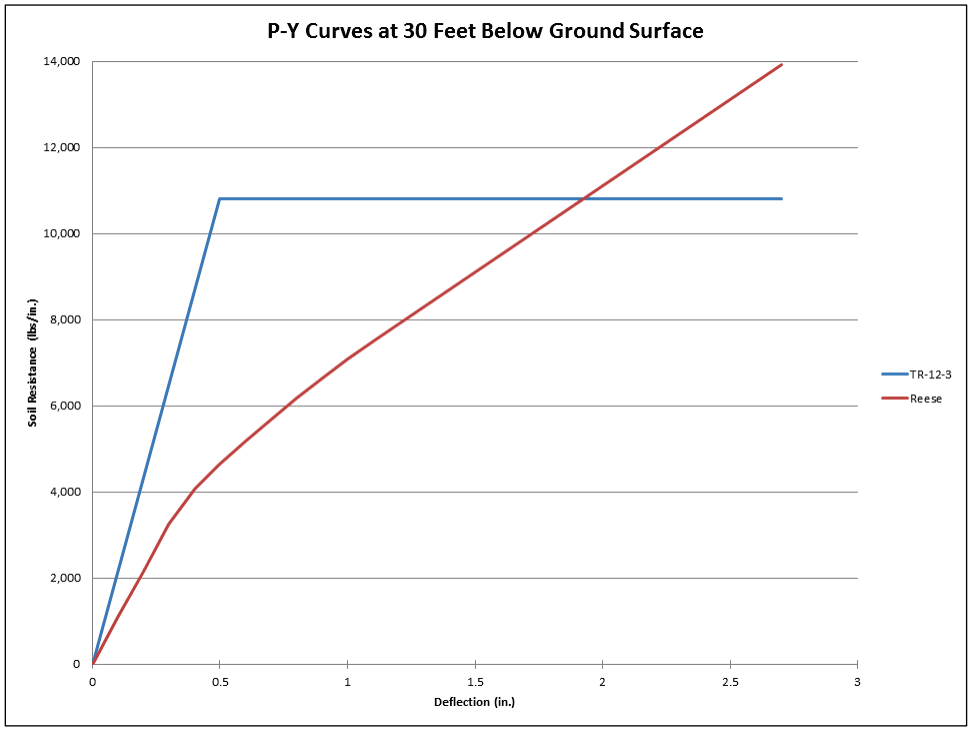

Figure 2.7. Comparison of Reese sand criteria p-y curves with the p-y curves used in Ebeling et al. (2012) at 59 ft depth below the mudline.

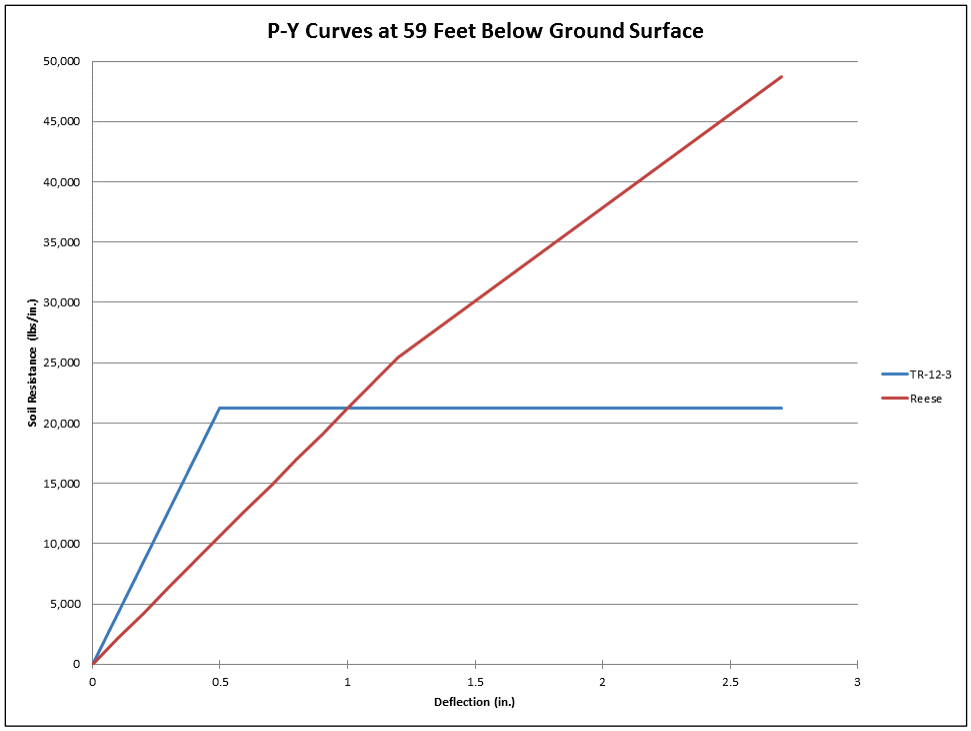

Figure 2.8. Comparison of the Reese p-y curves at different depths below the mudline in sandy soils (where pressures vary with depth).

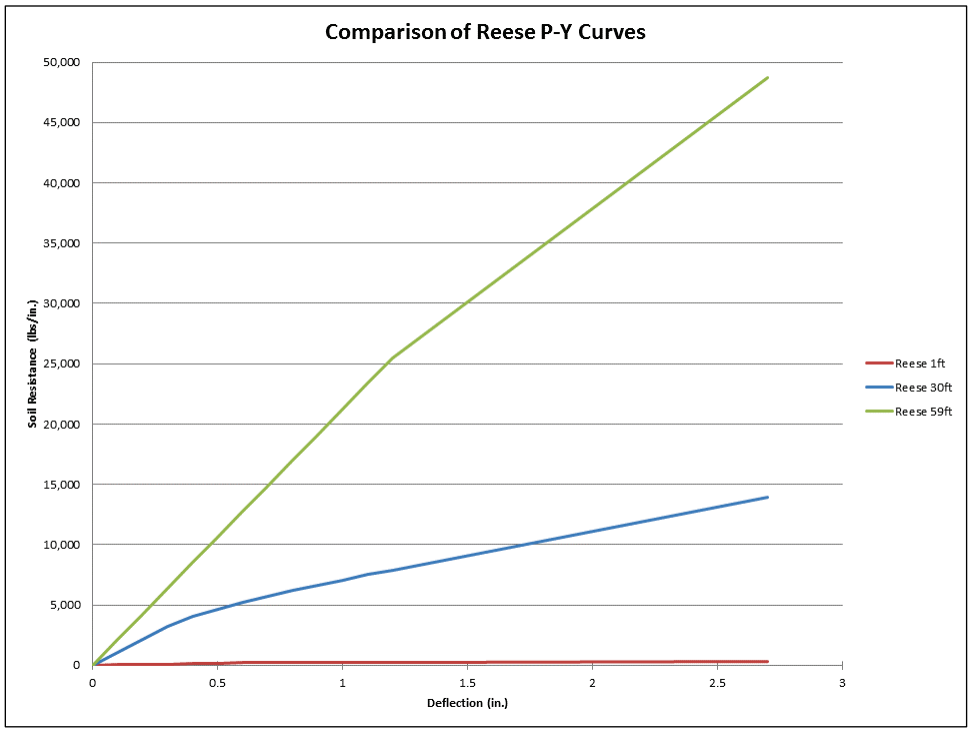

The user-defined p-y curves from Ebeling et al. (2012) seem to be very different from the Reese sand criteria p-y curves for the same depths. It could be assumed prior to conducting a COM624G analysis that these curves would give very different deflections at the pile cap for the same pile subjected to the same lateral load. Figure 2.9 shows the pushover curves derived using the pushover process using COM624G as described above.[1]

Figure 2.9. Pushover curves for a single pile in the example 2-pile bent given different p-y curves.

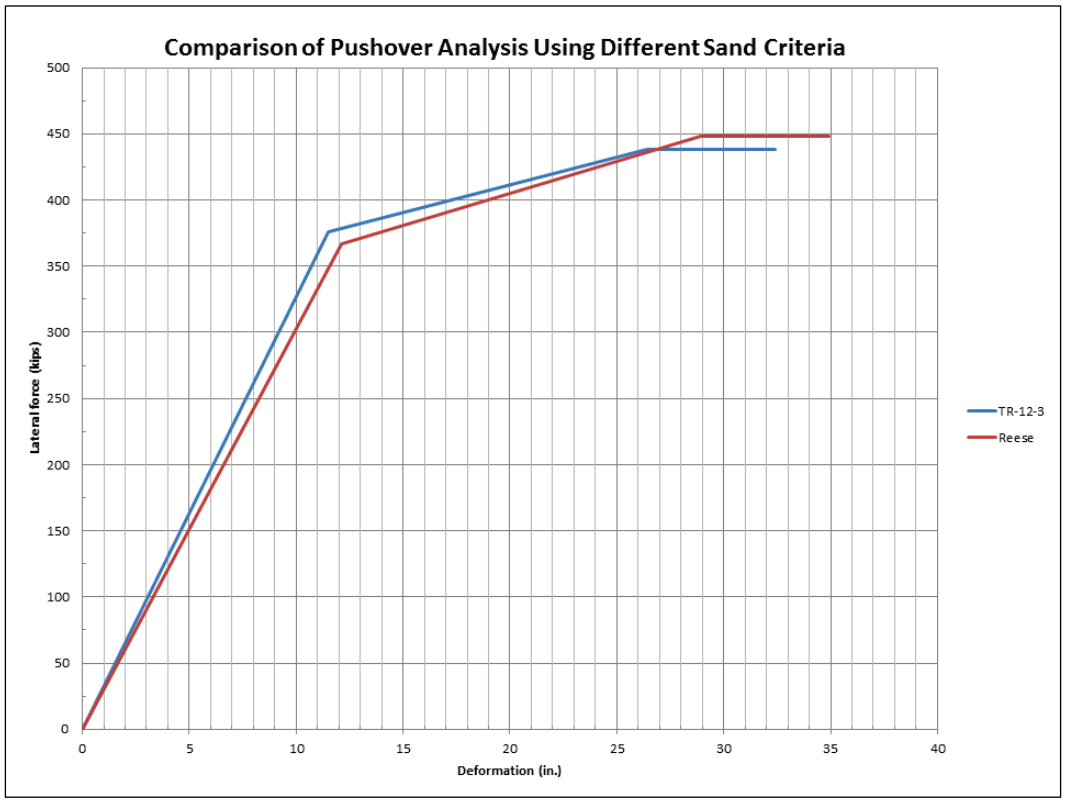

It turns out that the pushover curves from the two analyses are very similar. It is suspected that this agreement between the two Figure 2.9 p-y curve-based pushover analyses may be accounted for by the fact that the Relative Stiffness Factor (T), computed using Equation 2.2 as the fifth root of the ratio of EI to n_h, leads to small changes in value as n_h increases.

The resulting pushover curve data points (for a single pile) using M-PHI and COM624G are summarized in Table 2.2.

[1] For a two-pile clustered pile-group substructure, the vertical axis force values resulting from the pushover curve would be double those force values obtained for a single pile. The x-axis displacement values do not change when altering the pushover curve results from a single pile to account for a two-vertical-pile substructure.

Table 2.2. Pushover curves computed using two different sets of p-y curves for sand.

Ebeling et al. (2012) p-y curves		Reese Sand Criteria p-y curves	
Deformation (in.)	Force (lbs)	Deformation (in.)	Force (lbs)
0.0	0.0	0.0	0.0
11.0	376,470.0	12.1	367,000.0
26.6	446,000.0	28.9	448,000.0
32.6	446,000.0	34.9	448,000.0

Figure 2.10 shows the deflections of the piles under two different load levels: the load that starts the flexural hinging at the pile-to-pile cap (push-over analysis 1), and the greater load resulting in flexural hinging at a short distance below the mudline (pushover analysis 2). While the deflection of the pile at 1 ft below the mudline (492 in. below the pile cap) is significant, the deflections at 30 ft (360 in.) below the mudline (840 in. below the pile cap) and 59 ft (708 in.) below the mudline (1,188 in. below the cap) are fairly insignificant. Multiplying the greater deflection at 1 ft by the less stiff 1 ft p-y curve gives a value that is comparable to the multiplication of the lesser deflections at 30 and 59 ft to the stiffer p-y curves at those depths. This is why the pushover curves, at the pile cap, are similar for the COM624G p-y curves and the Ebeling et al. (2012) p-y curves.

Figure 2.10. Deflections along the pile for each pushover step (flexural hinging of the pile cap in blue, and flexural hinging at mudline in red).

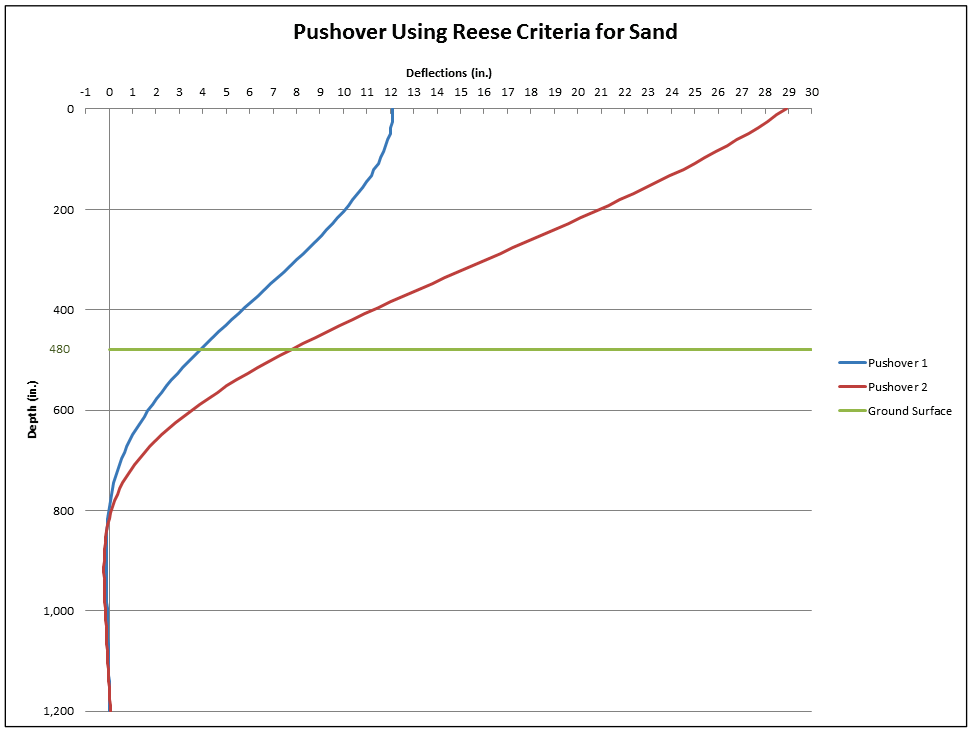

Figure 2.10 shows the resulting COM624G deflections along the pile for the pushover loads at the point (#1) when the pile cap loses moment capacity (in blue) and later when an even larger lateral load is applied (#2) and the pile hinges at a short distance below the mudline (in red). The mudline is shown as a horizontal green line. Observe the impact of the fixed-head boundary condition on the pile displacements at the pile cap (blue displacement curve); the pile displacement is perpendicular to the pile cap. The pinned-head, boundary-condition, pile-cap displacement results (red curve) do not possess this feature because the top of the pile is free to rotate.

Figure 2.11 shows the deflections of the pile under the first and second pushover loads from a depth of 720 in. (60 ft) to 1200 in. (100 ft) below the pile cap. The pile embedment range is from 20 ft to 60 ft. Notice that the deeper the pile embedment, the pile deflections begin to mirror each other. For instance, the first zero-deflection point depth is 792 in. (66 ft) for the first pushover load and a depth of 816 in. (68 ft) for the second pushover load, giving a difference of 24 in. The second zero-deflection point depth is at 1140 in. (95 ft) for the first pushover load and 1152 in. (96 ft) for the second pushover load, giving a difference of only 12 in. This trend continues with the depth of embedment of the pile and sets the stage for the asymptotic relationships to be discussed later.

For the pile analysis, we know that any factored load should not take the structural system beyond the point of flexural hinging at a short distance below the mudline. This can result in a structural mechanism being formed. In this example problem, the conservative estimate for factored loads is the ultimate moment capacity of the pile using the cracked moment of inertia at a short distance below the mudline, determined from a pushover analysis. Service loads are related to allowable stress design, which is not used for reinforced concrete structures; therefore, service loads are not considered in this report, other than in a discussion of state-of-the-practice techniques.

Table 2.3 shows that the factored load corresponds directly to the load that leads to flexural yielding at a short distance below the mudline. This is the assumption that takes the designer from the capacity-based design loads to the performance-based design loads, especially with respect to following rule-of-thumb, pile-tip depth methodologies.

Figure 2.11. Deflections along the pile for each pushover step for a section of the pile embedded in the soil (flexural hinging of the pile cap in blue, and flexural hinging at mudline in red).

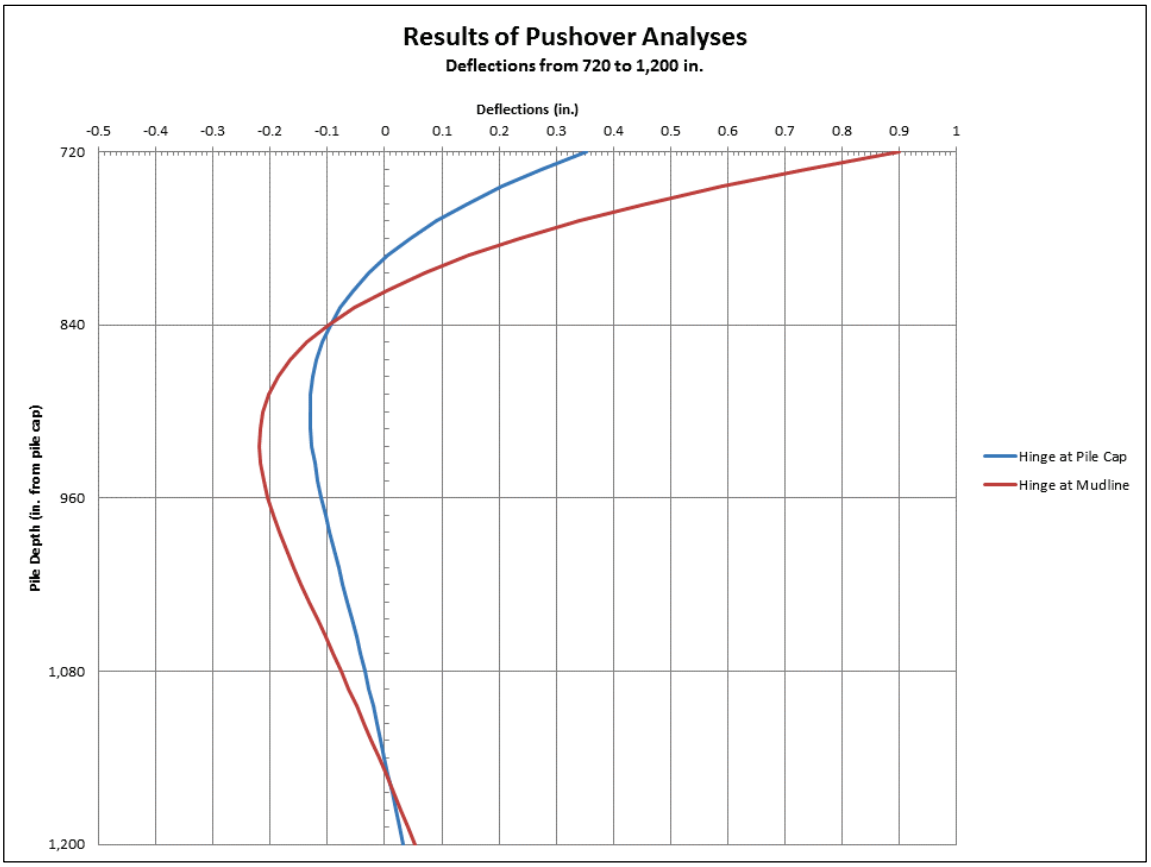

Table 2.3. Determination of factored loads.

	Ebeling et al. (2012) sand model	Reese criteria sand model
	Load (lbs)	Load (lbs)
Flexural yielding at pile cap	376,470.0	367,000.0
Flexural yielding at a short distance below the mudline	446,000.0	448,000.0
Factored Load	446,000.0	448,000.0

2.3 Going beyond Davisson for Pile-Embedment Depth

The following methods for determining how deep to embed a pile to achieve long-pile behavior were investigated by Lien (2011) and Reese et al. (1970). Each of these methods relies on information obtained from the deflection plot-versus-depth. These methods were developed for bridge piles and other piles with load conditions that are not used for navigation structures. In sections 2.3.1-2.3.4, these methods were investigated and modified to work with navigation load conditions.

2.3.1 Design length by second zero-deflection point under factored load conditions

The original version of this method (Lien 2011) was referred to as the second zero-deflection point for service load and was recommended in Wang and Reese (1993). This design method is for an allowable stress design of steel piles; there is no allowable stress design for reinforced concrete in design practice. Only strength design is used for reinforced concrete, so this method has been modified to use the factored load of Table 2.3 instead of the service load.

This method asserts that the depth of embedment for a pile exhibiting long-pile behavior occurs at the second zero-deflection point from the mudline. If a second zero-deflection point is not reached in the COM624G model, it may be necessary to extend the length of the pile for the pushover analysis. Figure 2.12 shows the deformations of the pile below the mudline (at 480 in. (40 ft) below the pile cap). The first and second zero-deflection points in our example problem are found at 817 in. (68.08 ft) and 1152 in. (96 ft) below the pile cap, respectively. The distances below the mudline for these two zero deflections are 28 ft (336 in.) and 56 ft (672 in.), respectively. The second zero-deflection point for this factored load method thus gives a depth of embedment for long-pile behavior as 56 ft (672 in.) of embedment. Recall that there is an additional 40 ft (480 in.) of exposed pile above the mudline. Lien (2011) mentioned that this method is conservative with regard to service load design. It is likely that using the greater factored loads for this method will continue to give conservative results.

Figure 2.12. An exaggerated scale view of how a pile deflects below the mudline given factored loads.

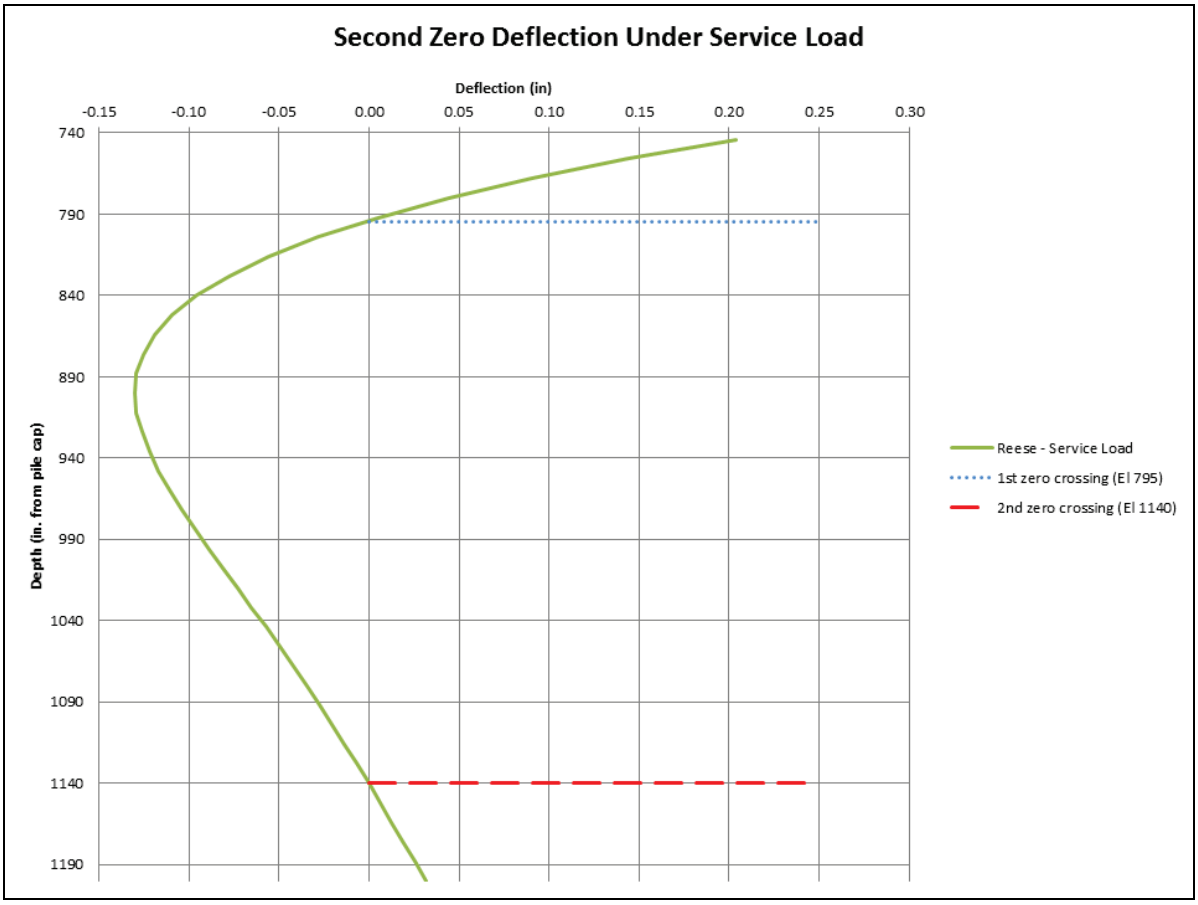

2.3.2 Design length by maximum negative-deflection point under factored loads

The second method, referred to as design length by maximum negative-deflection point under factored loads, applies the factored load to the pile and determines the shape of the deformed pile. Figure 2.13 shows the deformations from 740 in. (61.66 ft) below the pile cap to the pushover pile tip at 1200 in. (100 ft) below the pile cap. For reference, the first zero-deflection point with the factored loads is at 817 in. (68.08 ft) below the pile cap (or ~28.1 ft below the mudline). The maximum negative-deflection point, with a deflection of –0.22 in., is at 924 in. (77 ft) below the pile cap (or 37 ft (444 in.) below the mudline). Therefore, the pile-tip depth for long-pile behavior would be assumed to be 37 ft (444 in.) below the mudline by this method. Lien (2011) mentioned that this method is an acceptable method.

Figure 2.13. An exaggerated scale view of how a pile deflects below the mudline given factored loads.

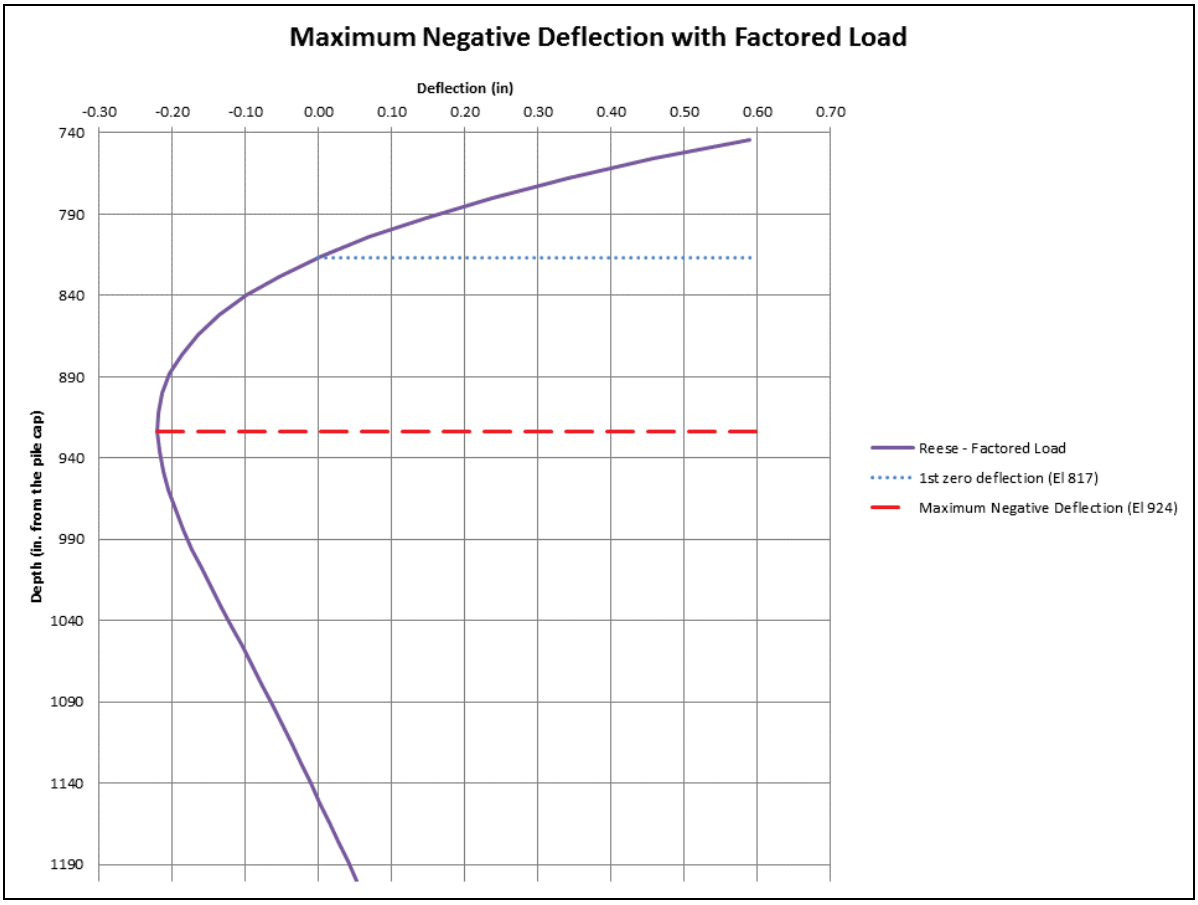

2.3.3 Asymptotic pile-cap deflection method

The third method, referred to as the asymptotic pile-cap deflection method, is more complicated than the first two methods. As in the previous two methods, the factored load is applied to the pile cap to determine the shape of the deformed pile. The analysis depicted in Figure 2.13 is also applicable here, with the zoomed-in plot showing the deformations from 740 in. (61.66 ft) below the pile cap to the pushover pile tip at 1200 in. (100 ft) below the pile cap. The first zero-deflection point with the factored loads is at 817 in. (68.08 ft) below the pile cap (or ~28.1 ft below the mudline). The maximum negative-deflection point, with a deflection of –0.22 in., is at 924 in. (77 ft) below the pile cap (or 37 ft (444 in.) below the mudline).

The asymptotic pile-cap deflection method postulates that the pile-tip depth for long-pile behavior lies somewhere between the first zero-deflection point and the point of maximum-negative deflection. In order to find this point, a set of COM624G analyses needed to be performed with

varying pile-tip depths (changing the pile length) using the same pile model and factored load. The pile-tip depths would start at the maximum negative-deflection point and go up to the first zero-deflection point. For each of these analyses, the pile deflections at the pile cap were measured.

Looking at the deflections shown in Figure 2.14 as a function of pile-tip depth which extended far below the maximum negative-deflection point, an asymptotic curve is revealed. The point at which the slope of the curve starts showing less pile-deflection at the pile cap per change of pile-tip depth in conjunction with engineering judgment can be used to define the pile-tip depth required to achieve long-pile behavior.

Figure 2.14. Variation of deflections at pile tip, mudline, and pile cap for piles of varying depth using the Reese criteria for sand.

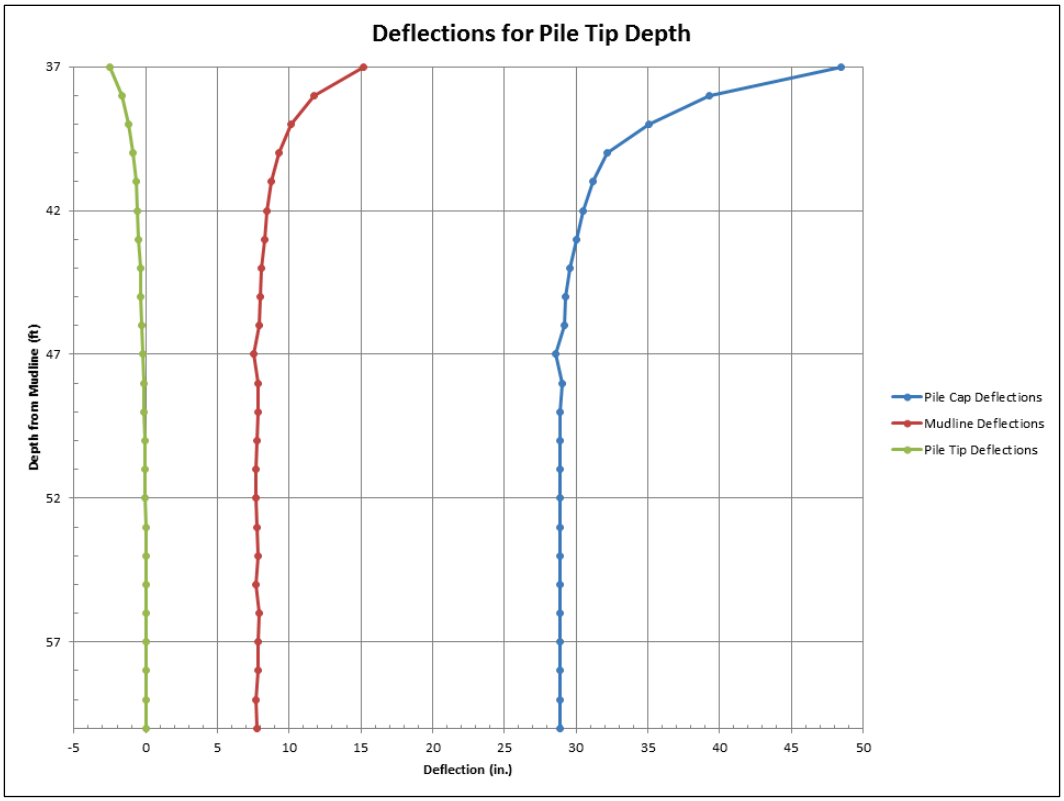

At this point, the pile-tip depth solution by the asymptotic pile-cap deflection method was discovered to have an issue. While COM624G could determine a pile deflection when the pile tip was set to the maximum negative-deflection point (37 ft (444 in.) below the mudline) for the estimated long-pile length (assumed 60 ft (720 in.) below the mudline), it was soon apparent that the pile-cap deflections were becoming more asymptotic as the pile-tip depth (and the pile length) was decreased. Although Lien (2011)

mentioned that this is another acceptable method, the range of values did not reveal the full asymptotic nature of the curve. The example problem evaluation revealed that the range of depths needed to be changed.

The asymptotic curve of Figure 2.14 did show improvement as the pile-tip depth was increased from 37 ft (444 in.) below the mudline to the second zero-deflection (under factored loads) of just over 55 ft (660 ft) below the mudline. The three curves for the computed deflections of the pile at the pile tip, mudline, and pile cap for different pile-tip depths are shown in Figure 2.14. The pile-tip deflections are shown in green, the mudline deflections in red, and the pile-cap deflections in blue. It appears that all of these curves seem to level out at a depth of about 43-47 ft (516-564 in.) beneath the mudline.

While the asymptotic pile-cap deflection method relies on engineering judgment to assess the point at which the pile achieves long-pile behavior using the curve of the pile-cap deflections over various pile-tip depths, it may be possible to define an angle (based on the change in deflection with change of pile-tip embedment) for the displacement-versus-depth curve at which long-pile behavior could be assumed. This is discussed further in a subsequent section.

2.3.4 Asymptotic pile-cap delta-deflection method

Reese et al. (1970) also recognized the asymptotic nature of the deflection for piles supporting breasting dolphins at a coastal project. The pile that they analyzed was a 54-in.-diameter steel tubular pile that extended 45 ft (540 in.) above the mudline. A lateral load of 175 kips was applied to the pile and pile-cap deflections were computed using a p-y curve-based procedure of analysis for pile-tip penetration depths (i.e., depth from the pile cap) the investigation ranged from 80 ft (960 in.) to 100 ft (1200 in.), where 100 ft is the estimated long-pile length. The asymptote of the pile-cap deflection curve had a deflection of nearly 16 in. The pile-tip minimum penetration was set at 86 ft (1032 in.) by the authors, which resulted in a deflection of 17 in. (1 in. greater than the asymptote), and implied that limits could be based on percentage change of deflection (6.25%) or just on a small relaxation in the deflection.

If a 1 in. change of deflection from the asymptote were set as the limit for the computed pile-cap deflection data in Figure 2.14, then the pile depth of embedment (below the mudline) for this example would be approximately

43 ft (516 in.). The pile deflections would go from 28.9 in. at the asymptote to 30 in. at 43 ft.

Because deflection is highly dependent on the properties and size of pile as well as the magnitude and the height of the lateral design load, it may be better to work with a percentage of the deformation as a limit. Reese et al. (1970) had a deformation percentage of 6.25% (e.g., 1 in. change from the asymptote at 16 in.). When applied to the asymptote of the authors' example (e.g., 28.9 in.), this corresponds to 1.8 in. change of deflection. This change in deflection from the asymptote occurs at approximately 42 ft (504 in.) depth of embedment.

2.4 The Budek et al. (2000) depth of embedment criteria

Budek et al. (2000) required a depth to establish nodal fixity at the pile tip in a finite element model of a pile embedded in soil that uses the Winkler spring model for soil stiffness. Budek chose the depth of the pile to allow "pile" (not "pole") behavior, which he specifies as pile-tip displacements that are less than 0.001 times the pile-head displacement. Recall that pole behavior occurs when the loaded pile ploughs through the surrounding soil. This "depth to equivalent fixity for displacement" as named by Budek,[1] is based on the asymptotic deflections of the "head," or pile cap, and the pile tip in an iterative search using increasing pile-tip embedments. Therefore, his search for pile behavior is functionally equivalent to the Reese et al. (1970) method to determine long-pile behavior, with a different displacement criterion given by:

$$0.001 > \frac{d_{piletip}}{d_{pilecap}} \tag{2.5}$$

Figure 2.15 shows the results of computing the ratios of pile-tip deflections to the deflections at a short distance below the mudline and at the pile cap. The absolute value of the pile-tip deflection is used because the pile-tip deflections were gathered from the maximum negative pile-tip deflection to a point below the second zero-deflection point of 1152 in. (96 ft) depth (Figures 2.12 and 2.13) or 56 ft (672 in.) embedded depth. While the ratio of the deflections does seem to follow an asymptotic curve, the curve itself doesn't seem to give any information about pile-tip depth for long-pile behavior, other than the second zero-deflection point (where the numerator of the ratio goes to zero at approximately 55-56 ft (660-672 in.). In fact, the

[1] The depth to equivalent fixity for displacement is also referred to as the point of effective fixity in Budek.

pile-tip deflection drives the convergence of the ratio to the zero value. The ratio between pile-tip deflection to pile-cap deflection reaches the suggested Budek limit of 0.001 with a pile-tip depth below the mudline of 53 ft (636 in.).

Figure 2.15. Budek ratios for the pile-tip deflection per mudline deflection and per the pile cap deflection.

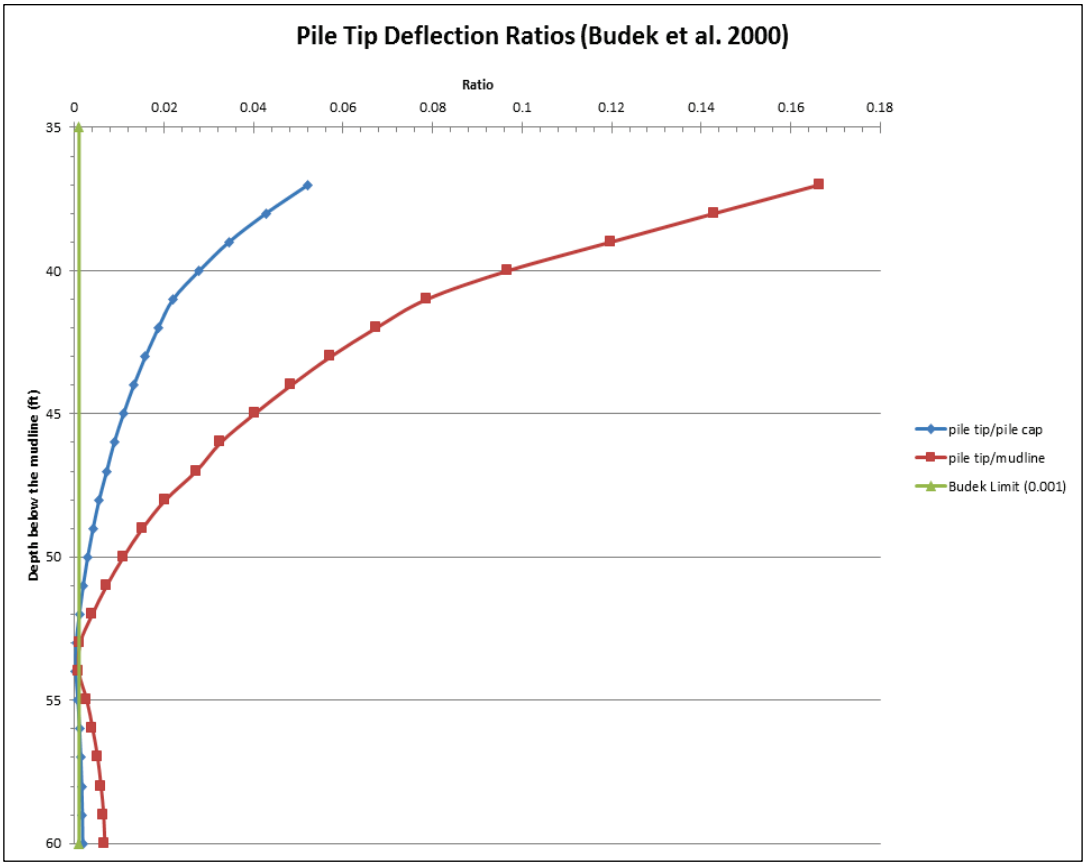

The Budek limit establishes a depth range that will be acceptable for pile depth that is roughly coincident with the second-zero deflection point. Changing the limit adjusts the range and affects how liberal this change will be. Making the range broader than 0.001 by say a factor of ten (i.e. equal to 0.01) will result in shorter pile length, and making the range narrower will result in longer pile lengths approaching the second-zero deflection point (with a ratio of 0.0).

2.5 Asymptotic curves for change in deflection versus change in pile tip depth of embedment

Recall that Reese et al. (1970) suggested a deflection of 1 in. for the 45 ft (540 in.) exposed pile section that they were working with, or 6.25%

greater than the long-pile deflection. Budek et al. (2000) suggested that since the pile-cap deflections were related to the pile-tip deflections, a limit could be applied to the ratio of pile-tip to pile-cap deflections, but the specified limit was very conservative. However, the idea that the pile tip was related to the definition of long-pile behavior suggested another method for determining pile-embedment depth for long-pile behavior. Because the pile-tip deflection is related to the pile-cap deflection, as related by the Budek et al. (2000) procedure, and the pile-tip deflections are minimal about the placement of the pile tip, then long-pile behavior can be considered to occur as the pile-tip deflections approach zero.

As shown in Figure 2.14, the deflections at the pile cap, pile tip, and at a short distance below the mudline for the pile are shown with respect to the changing pile-tip depth of embedment. The change in deflection with respect to the change in pile depth can be computed, and this derivative value gives the rate of change at which the curves are stabilizing for long-pile behavior.

Figures 2.16-2.18 show the derived values of the three slope-of-deflection curves with respect to the pile-tip depth. Because the rate of change for these slope-of-deflection curves shows a definite inverse value relationship between the pile-cap deflection rate of change and the pile-tip deflection rate of change, the values of the pile-tip curve have had their signs inverted in Figure 2.16. The mudline deflection rate of change is actually more variable, likely due to changes in the depth of the pile-to-peak moment, since the factored load applied in the analysis is near the point of pile hinging. Although the horizontal scales are different for each curve, the shapes of the curves are very similar.

Because these plots are based on asymptotic deflection curves, the derived values for the slope of the deflections as the pile-tip depth is increased are also asymptotic. However, these plots also reveal a definite inflection point where the pile tip begins to mobilize the soil. At this point, the rate of change of deflection begins to show nominal change as the pile-tip depth is increased. This same behavior should exist for piles in any homogeneous, cohesionless soil.

From Figure 2.16, the inflection point can be seen to occur when the slope of the deflections per pile depth has a value of 0.01. This occurs when the pile depth is near 42 ft (504 in.) in depth. Figures 2.17 and 2.18 show that this same inflection point with depth of 42 ft (although the slope is different) is apparent for the mudline and pile-cap deflection slope curves.

Figure 2.16. Derived values for change of pile-tip deflection for 40’ exposed pile.

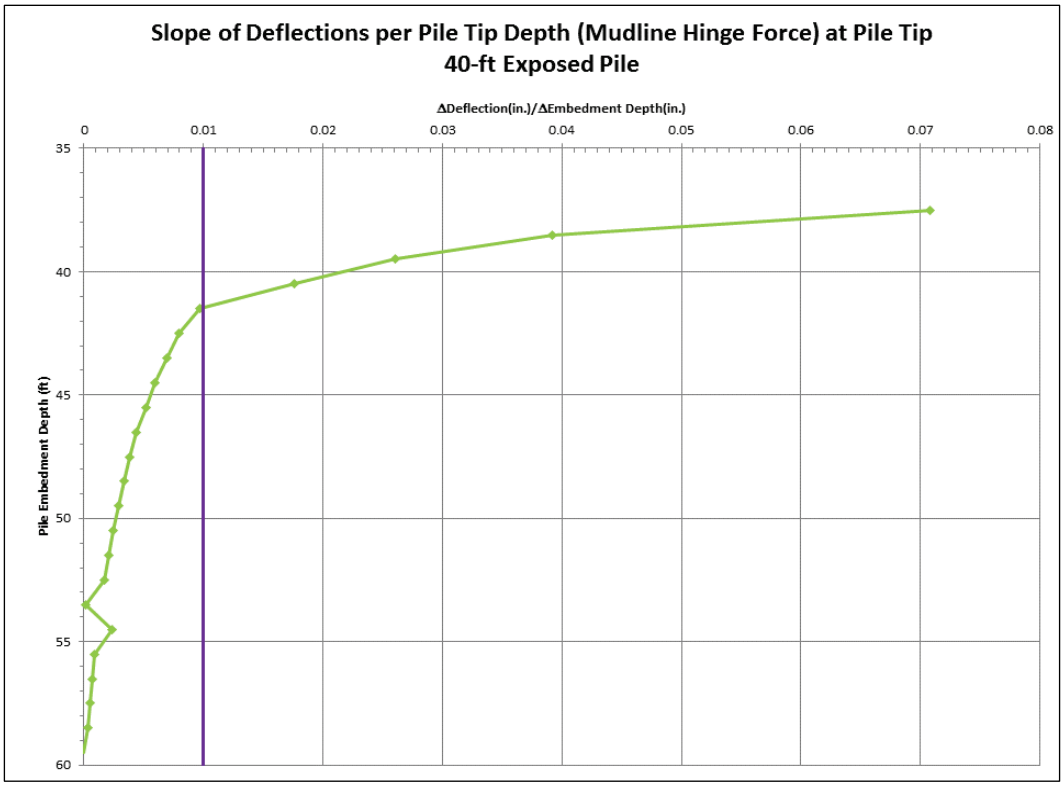

Figure 2.17. Derived values for change of mudline deflection to change in depth for 40’ exposed pile.

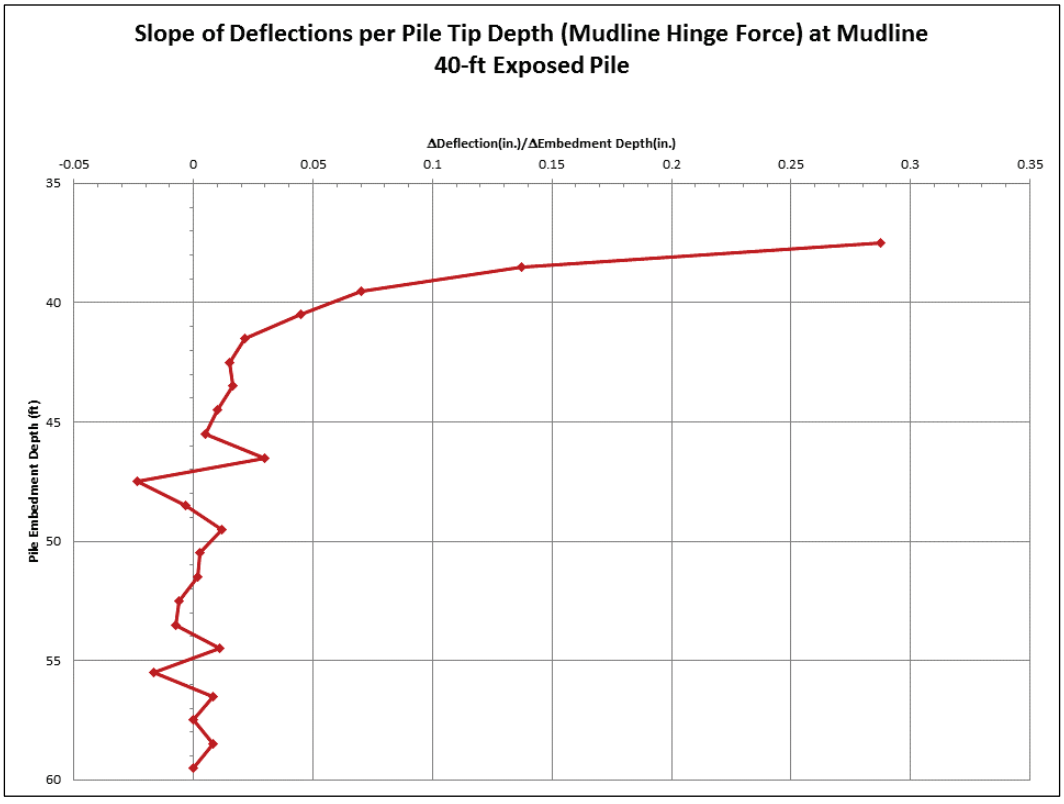

Figure 2.18. Derived values for change of pile-cap deflection to change in depth for 40' exposed pile.

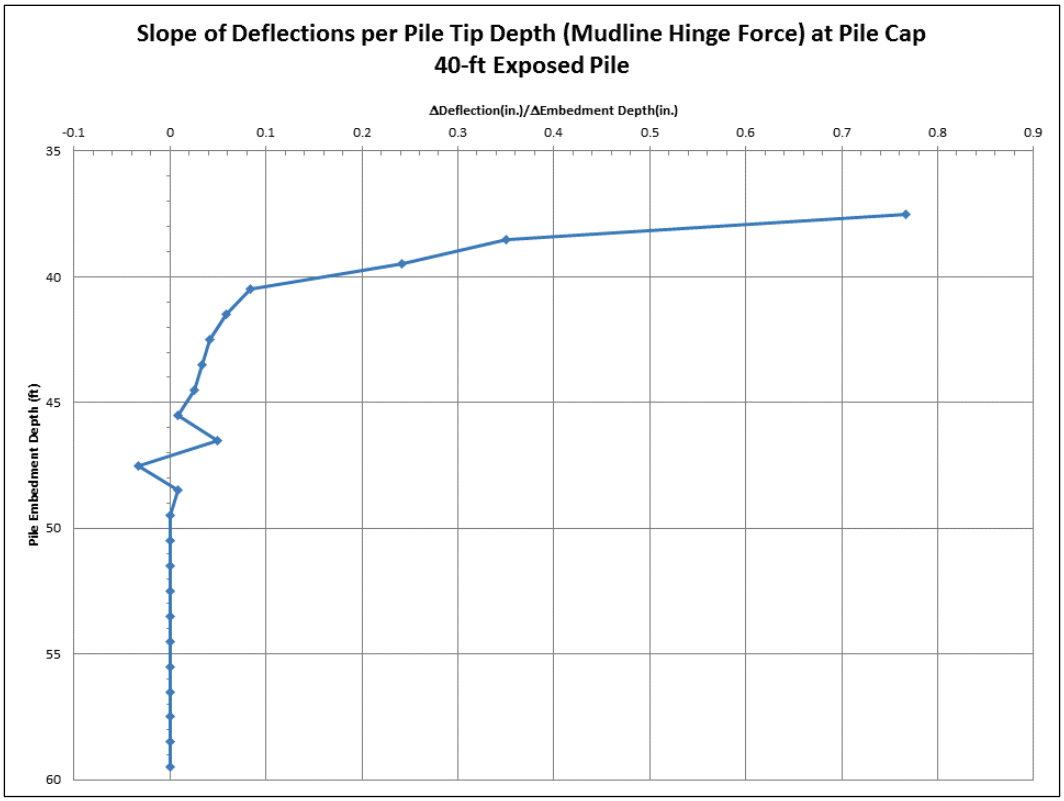

This value represents the point where deflections show a marked difference in the rate of change of behavior of the pile in the soil under a lateral load, so the authors of the report suggest that this inflection point is the most reliable indicator of long-pile behavior. Because of the variation of the derived values for the calculations made at the mudline, the smoother curves made for the pile tip and the pile cap are deemed more reliable for interpretation. Furthermore, because the deflections and their slopes are smaller at the pile tip, yet still related to pile-cap deflections and their slopes, this set of values is more stable for analysis and more reliable for inflection-point analysis.

2.6 Comparing pile-embedment depth for the first pushover load (pile-cap hinge) as compared to the second pushover load (mudline hinge)

Up until this point, it was assumed that the deepest depth of embedment to assure long-pile behavior occurs when the ultimate capacity leading to the collapse of the pile-bent structure is reached in a pushover analysis. However, this assumption did not take into account that the fixity condition

at the pile cap affects the movement of the pile at greater depths (i.e., affecting what Yang 1966 refers to in his Figure 2 as the effective embedment depth). The altered movement the pile (due to fixity at the pile cap) may result in a deeper depth of embedment to reach long-pile behavior than the pinned condition for the second stage of the pushover analysis. Therefore, the best course of action will be to find the depth of embedment assuring long-pile behavior at each load case of the pushover analysis. The greatest depth assures long-pile behavior for all of the load cases.

At each incremental load case of a pushover curve, the asymptotic deflection response of the pile tip should be measured as the pile-tip depth is increased. For the example problem pushover with a 40 ft (480 in.) exposed section of pile, Figure 2.19 shows the values of deflection for the first flexural yield point load (pile-cap hinge) and the second flexural yield point (mudline hinge).

Figure 2.19. Comparison of pile-tip deflections for the pushover load cases.

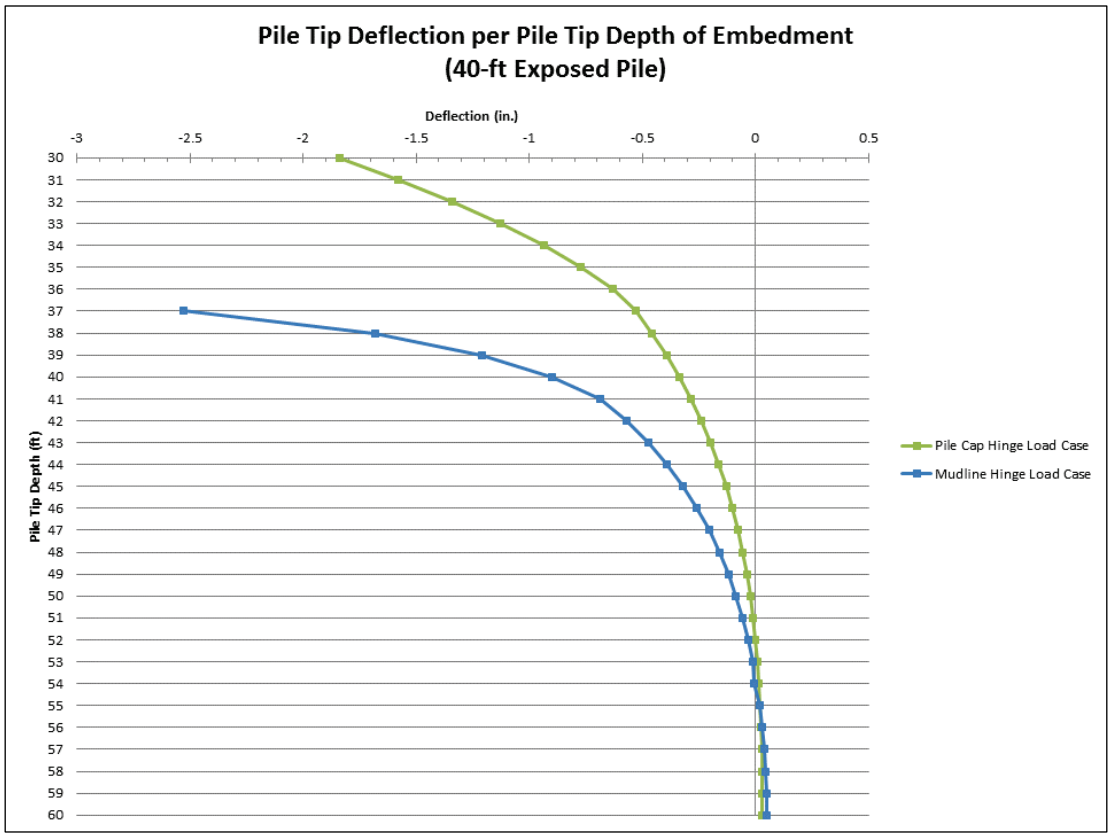

Figure 2.20 shows the change of pile-tip deflection with respect to the change of pile-tip depth (computed for each pile-tip depth) for the first and second flexural yield point loads. The inflection point for the first flexural yield point load (pile cap hinge) as the pile tip approaches a 38 ft (456 in.) embedment. The inflection point for the second flexural yield point load (mudline hinge) as the pile tip approaches a 42 ft (504 in.) embedment. Because the change in pile-cap deflection (which is used to define long-pile behavior) has nominal change as the pile-tip depth increases, the deeper pile depth is the one to be specified based on the results from the pushover analysis. In this case, the second flexural yield load (mudline hinge) requires a 42 ft depth of embedment for long-pile behavior. This depth would also satisfy the long-pile behavior requirement over the whole pushover process.

Figure 2.20. Comparison of pile-tip inflection points from derived values for the pushover load cases.

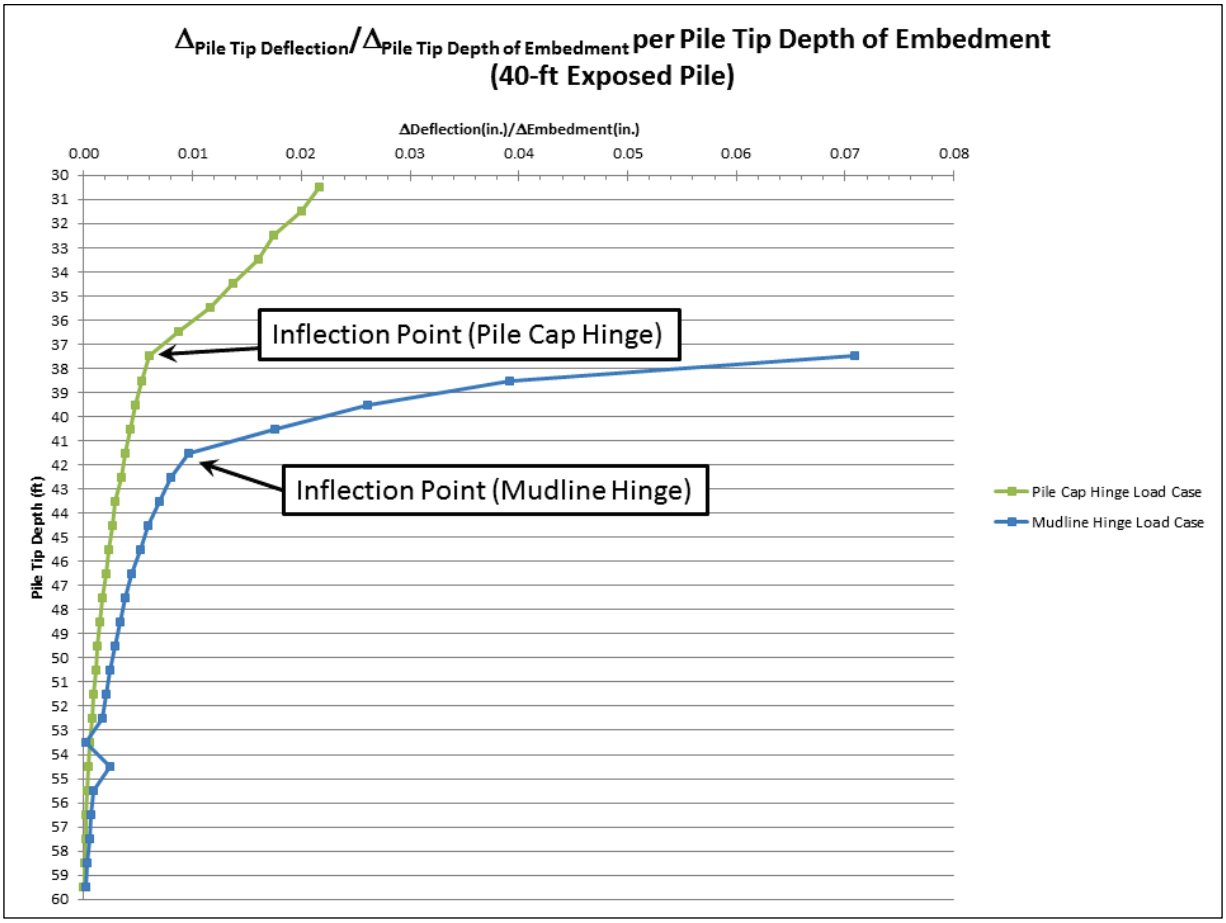

2.7 Long-pile behavior embedment results for 40 ft vertical exposed piles

The primary design load for lock approach walls are barge train impacts on a beam or deck. The primary loading is transverse to the line of the approach wall. Pile-founded flexible lock approach walls are typically constructed with impact beams simply supported on pile bents or by using an impact deck supported by groups of clustered piles. These bents and decks are supported tens of feet above the mudline. Barge impacts occur at the beam or deck level (i.e., lateral loading at the top of the pile). Because of this lateral loading at the pile cap, vertical pile groups must be designed to exhibit long-pile behavior (e.g., minimal change in deflection at the pile cap with an increased depth-of-pile embedment). These lateral design loads at the top of the pile introduce substantial moments for the vertical piles at a short distance below the mudline. Methods for estimating the minimal vertical pile-tip depth of embedment giving long-pile behavior are investigated and improvements are suggested. Reducing the length of piles will result in a cost savings for Corps projects, especially for in-the-wet construction.

The results of the six different methods found in research for determining a pile-tip depth for long-pile behavior are presented in Table 2.4, as well as three altered asymptotic pile-cap deflection methods, where bounds and limits of the analysis were changed. These nine methods resulted in pile-tip depths of embedment ranging from 37-55 ft (444-660 in.).

The Davisson method and design length by maximum negative-deflection point under factored loads have a much shallower, liberal pile-tip depth than the other methods. In fact, according to Figure 2.14, these pile-tip depths will not allow for long-pile behavior at all, as they may allow the pile cap to deflect what might be characterized by some as an excessive amount. The authors of this report have been puzzled by this observation. Then it was realized that the methods discussed by Davisson and Lien seem to be applied to piles that do not have an extensive above-the-mudline exposed section of pile with large lateral (barge train impact) loading applied to the top of the extended pile. The moment introduced at a short distance below the mudline due to the exposed section of pile means that long-pile behavior will occur at greater pile-tip depths of embedment than piles capped at a short distance below the mudline. It should be noticed, however, that the design length by the second zero-deflection point for factored load procedure is conservative. This leads the authors of this report to suspect

that any long-pile behavior will occur in the range above the second zero-deflection point using factored loads and below the first zero-deflection point using factored loads (28-56 ft or 336-672 in.).

Table 2.4. Resulting pile depths for long-pile behavior using the different methods.

Method	TR-12-3 sand criteria		Reese criteria for sand		Notes
	inches below mudline	feet below mudline	inches below mudline	feet below mudline	
Davisson (D=4T)	472.8	39.4	472.8	39.4	T=118.2 (Ebeling et al. 2012, pg 121)
Design length by the 2nd zero deflection point for factored load	624.0	52.0	672.0	56.0	
Design length by maximum negative deflection point under factored loads	408.0	34.0	444.0	37.0	
Asymptotic pile cap deflection method	NR	NR	NR	NR	This method defined a result in the range 37ft > pile depth > 28ft An asymptote for the example pile was not found in this range
Altered asymptotic pile cap deflection method	NR	NR	516.0	43.0	From engineering interpretation
Asymptotic pile cap delta deflection method	NR	NR	516.0 504.0	43.0 42.0	Δdeflection = 1 inch %deflection = 6.25% (1.8 inches)
Altered asymptotic pile cap deflection method using Budek limit (pile tip deflection/pile cap deflection <0.001)	NR*	NR*	624.0	52.0	From Figure 2.15
Asymptotic pile tip deflection slope per pile tip embedment inflection point method	NR*	NR*	504.0	42.0	With an observed inflection point slope value of 0.01 (in/in) for the example

*No Results were recorded (at this time)

The asymptotic pile-deflection methods give the best definition of long-pile behavior, because the asymptote (as shown in Figure 2.14) reveals that there is a point at which further pile embedment has little impact on lateral deflections. A majority of the asymptotic methods give a range in pile-tip depths from 42-46 ft (504-552 in.). These asymptotic methods are less conservative than the 56 ft (672 in.) depth resulting from the second zero-deflection point for factored load procedure.

Figure 2.21 shows the depths of pile-tip embedment from Table 2.4. The pile-tip depths are shown with the asymptotic deformations computed for the pile tip, pile cap, and mudline of the pile. Where possible, methods that relate directly to the pile tip and pile cap are shown with their arrowheads touching the pile-tip and pile-cap curves.

Figure 2.21. Comparison of methods for computing the pile-tip depth for long-pile behavior using Reese sand criteria results for 40' exposed pile.

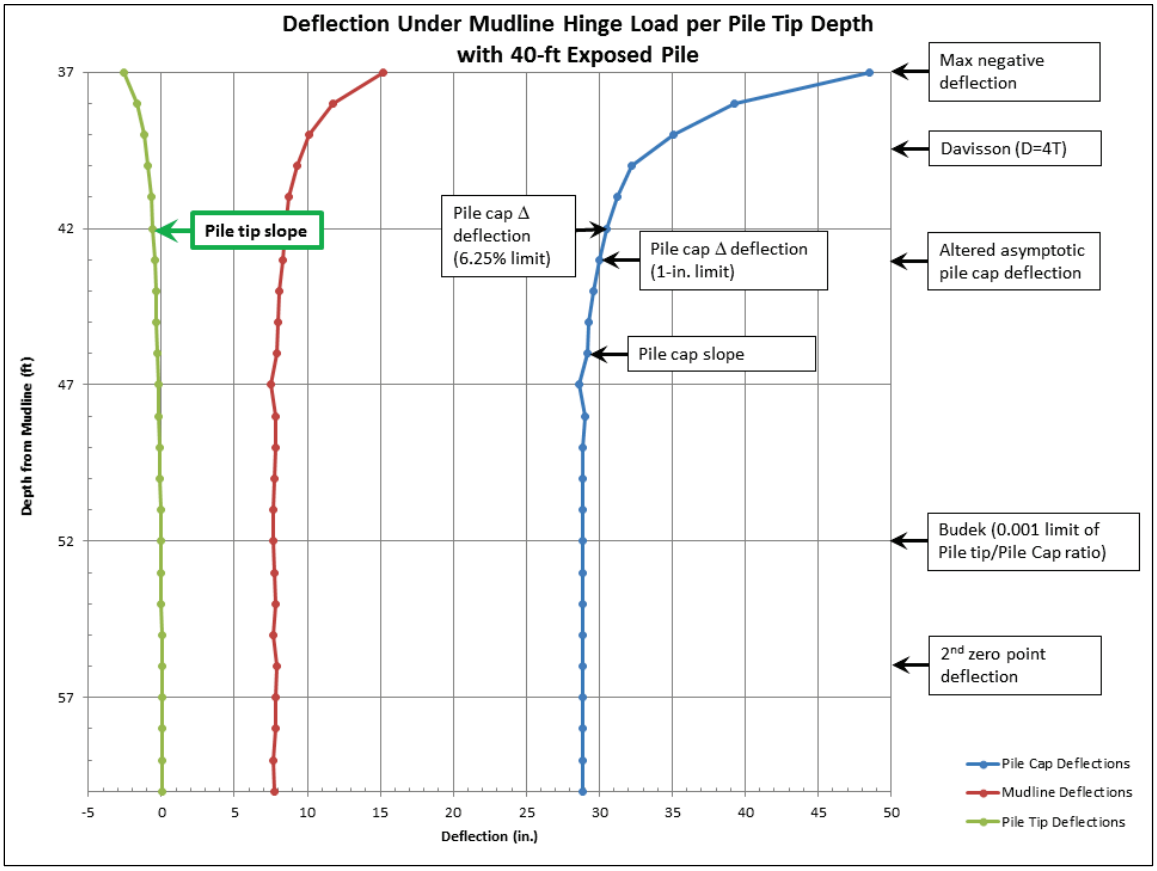

From the fact that minimal deflections occur with a pile-tip depth of more than 47 ft (564 in.), it is evident that the Budek and second zero-deflection point methods are very conservative methods. Likewise, the pile-cap

deflections for pile-tip depths of less than 40 ft (480 in.) are much greater than the minimal limit pile-cap deflection of 28.9 in.[1] For the maximum negative-deflection method, the deflection is 48.5 in. (4 ft), which is 68% greater than the 28.9 in. base deflection limit as interpreted by the authors. For the Davisson (D=4T) method, the deflection is 34 in. (2.83 ft), or 18% greater than the 28.9 in. base deflection limit. For the pile problem investigated, the resulting additional pile-cap deflection does not meet the definition of long-pile behavior that the authors introduced earlier.

As previously mentioned, the remaining five methods have resulting pile-tip depths that range from 42-46 ft (504-552 in.). One of these methods, the altered asymptotic pile-cap deflection method, is based on engineering experience that may not be readily available. Two methods are based on limits of pile deflection allowed at the pile cap. The final two methods are based on finding the point of curvature change based on the derived values of the change of deflections at the pile tip and the pile cap as the pile-tip depth increases.

The rate of change of the pile-tip deflections as the pile-tip depth increases is inversely correlated to the pile-cap deflection. Figures 2.16 and 2.18 show the correlation and the existence of an inflection point with respect to the curve of the change of deflections with respect to the pile-tip depth of embedment. With the small scale of deformation at the pile tip as compared to the larger scale of the pile-cap deformation, the authors believe that setting a limit (0.01) at the inflection point on the derived values of pile-tip deflections per pile-tip embedment would yield better results than any of the other methods.[2] The resulting pile-tip depth is shown in Figure 2.21 as a green box and arrow with bold text.

2.8 Long-pile behavior embedment results for 20 ft vertical exposed piles

In order to determine the effects that the exposed portion of the pile has on the pile-tip embedment depth for long-pile behavior, a second analysis was executed using the author's preferred method (discussed at the end of Section 2.6) with the same example pile problem, with the exception that the exposed section of the pile was reduced from 40 ft to 20 ft (480 in. –

[1] This 28.9 inch pile-cap deflection (as shown in Figure 2.21) corresponds to long pile behavior.

[2] This method is labeled as the asymptotic pile-tip deflection slope per pile-tip embedment inflection point method for the mudline hinge load case in Table 2.4.

240 in.). This had two major effects: the axial load (for the confining pressure in the pile) at a short distance below the mudline for an individual pile was reduced from 1130 kips to 1044 kips, and the moment arm for the load to the mudline was halved. The reduction in axial load confining pressure means that the shorter pile will not be able to withstand double the load, even though the moment arm is reduced to half its former value.

Figure 2.22 shows the resulting pushover curve for the single pile in this less-exposed pile system.[1] Recall that the force at mudline hinging for the 40 ft exposed pile was 448 kips. For the 20 ft (240 in.) exposed pile, the force at mudline hinging increases to 721 kips. The deformation at the pile cap of the 40 ft (480 in.) exposed long pile at collapse was 35 in. as compared to 24.6 in. for the 20 ft exposed pile. The deflection before mudline hinging at the peak load for the 40 ft long pile was 28.9 in., and the deflection before mudline hinging at the peak load for the 20 ft long pile was 18.6 in.

[1] For a two-pile clustered pile-group substructure, the vertical axis force values resulting from the pushover curve would be double those force values obtained for a single pile. The x-axis displacement values do not change when altering the pushover curve results from a single pile to account for a two vertical pile substructure.

Figure 2.22. Pushover curves for a single pile in the example 2 pile bent with 20' exposed piles.

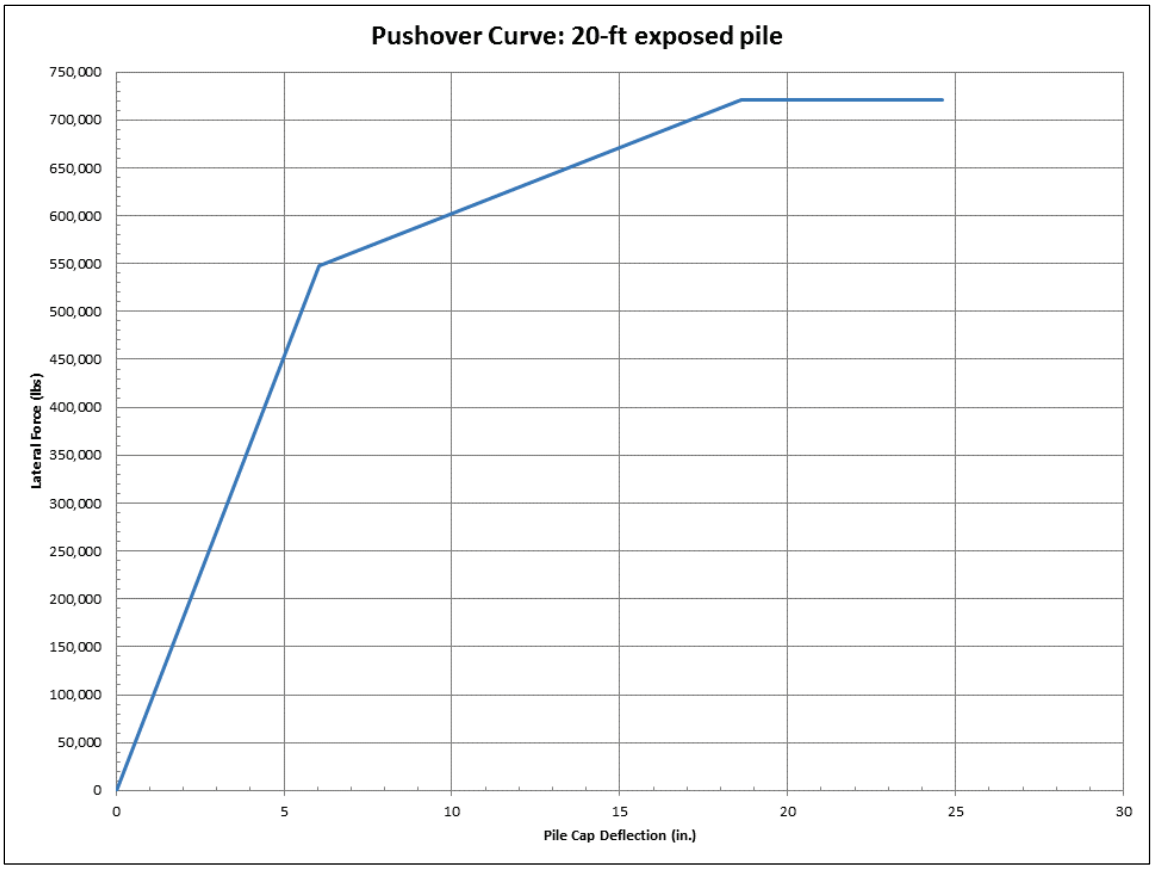

Figures 2.23 and 2.24 show the deflections of the piles with respect to pile-tip depth of embedment and the derived values of the change of deflection with respect to the change in pile-tip depth, respectively. The greater pile-tip depth of embedment for long-pile behavior of the two flexural yield loads and fixity imposed at the pile cap is the pile depth of embedment for long-pile behavior for the pushover analysis. Figure 2.24 also shows the limit at the inflection point for the derived value curve. It is interesting to note that these graphs have a similar range to the 40 ft (480 in.) exposed graphs for long-pile behavior, and that the inflection point for the 20 ft (240 in.) exposed pile is actually 2 ft deeper than for the 40 ft exposed pile. For the 20 ft exposed pile, the pile-tip depth for long-pile behavior is 44 ft[1] (528 in.) (conservatively rounding up the depth magnitude) and the 40 ft exposed pile has a pile-tip depth of 42 ft (504 in.) to long-pile behavior.

[1] As determined by the asymptotic pile-tip deflection slope per pile-tip embedment inflection point method, applied to the data contained in Figure 2.24 for the mudline hinge load case.

Figure 2.23. Variation of deflections at pile tip for piles of varying depth using the Reese criteria for sand for a 20' exposed vertical pile for the two pushover ultimate yield-point loads.

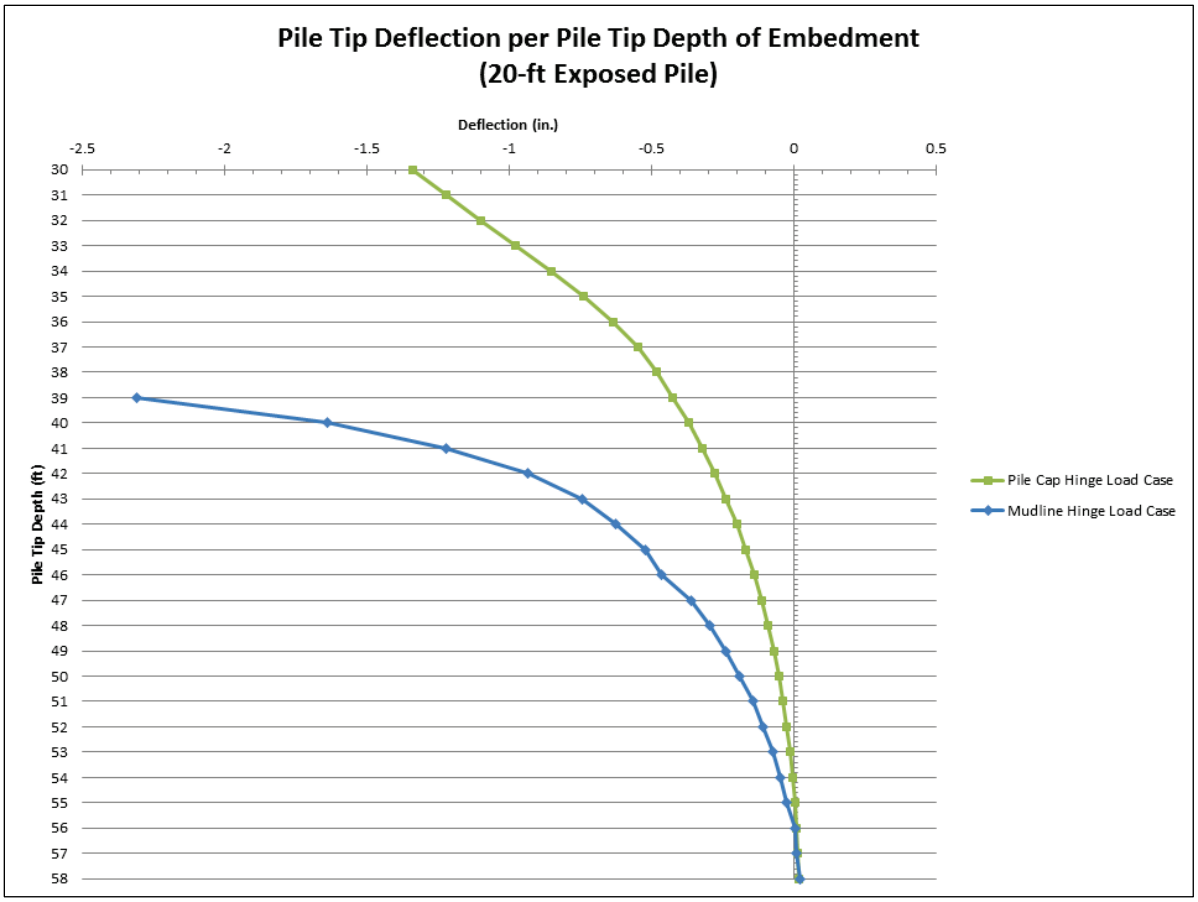

Figure 2.24. Derived values for change of pile-tip deflection to change in depth for 20' exposed pile for the two pushover ultimate yield-point loads.

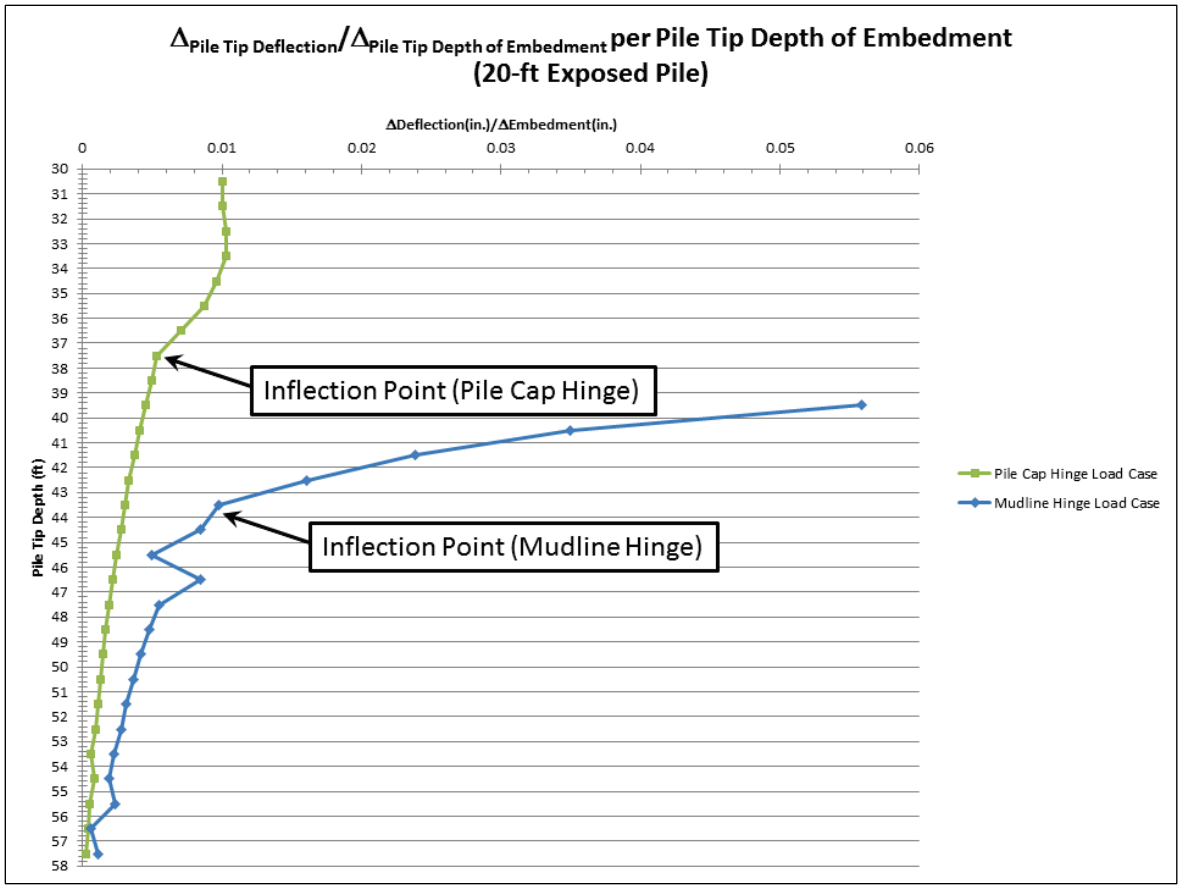

These results imply that long-pile behavior is largely dependent on the soil and pile properties other than the exposed length of the pile, but that the exposed length can affect the depth for a pile tip that will guarantee long-pile behavior.

2.9 Summary

In this chapter, a pushover analysis was performed on an example pile-bent system with two piles founded in a cohesionless sandy soil given two exposed heights (40 ft and 20 ft) and with an excessive pile-depth embedment. The pile-to-cohesionless sand soil-structure interaction was modeled with p-y curves and the Reese sand model. The pushover determined the peak force that could be applied to the approach wall section before the piles supporting the wall would yield at a short distance below the mudline and no longer support the impact loading applied to the approach wall. This would occur in an iterative procedure in the design process of the flexible approach wall.

It has been recognized that as piles are embedded deeper in the soil that the deflection at the top of the pile under a horizontal (impact) load is reduced, but that this deflection reduction hits a point of diminishing returns for deep pile-tip embedments. This property leads to the definition of long-pile behavior in this report. In order to reduce the costs associated with pile placement, the least embedment depth of designed piles that exhibits long-pile behavior needs to be computed. State-of-practice methods are established in the technical literature to estimate this depth of long-pile behavior. This chapter examined these state-of-practice methods and recommended a new course of action based on the pushover peak load.

The procedure recommended by the authors of this technical report used the peak force before hinging of the pile at a short distance below the mudline, and subsequent analyses to determine derivation of the slope of deflection at the pile tip versus the pile tip change-of-depth as the pile-tip depth of embedment increases. This procedure is referred to as the asymptotic pile tip deflection slope per pile tip embedment inflection point method. For the example pile with two exposed heights in cohesionless soil, each analysis revealed the existence of an inflection point that occasioned the beginning of long-pile behavior in the asymptotic pile-cap deflection curve. For 40 ft (480 in.) exposed height of pile in the example problem, the inflection point occurred with approximately 42 ft (504 in.) of embedment; for 20 ft (240 in.) exposed height, the inflection point occurred with approximately 44 ft of embedment.

The Davisson state-of-practice method ($D=4T$ for cohesionless soils, like sand) does appear to take the exposed length of the pile (above the mudline) into account. It simply applies a rule-of-thumb scale (4.0) to the "stiffness" (T) of the pile and cohesionless soil. For the example pile with the peak force applied at the 40 ft (480 in.) high top of pile, the result of applying the Davisson method was a pile-tip depth of 39.4 ft (472.8 in.), allowing a pile cap deflection of 35 in. rather than the 28.9 in. for long-pile behavior. For the 20 ft (240 in.) exposed pile and its peak load for mudline hinging, the deflection at the pile cap was 30 in., which still exceeds the 28.9 in. for long-pile behavior. For these example problems with the same cross-section pile and soil properties, the 4.0 scale factor for T of Davisson was liberal. From the results of the asymptotic pile-tip deflection slope per pile-tip embedment inflection point method preferred by the authors, the depths of the pile tip should be 42 ft (504 in.) for the 40 ft (480 in.) exposed pile, which is 4.26 * T, or 44 ft (528 in.) for the 20 ft exposed pile,

which is 4.47 * T. Because pile properties and soil materials at different sites have different properties, universally applying these new scale factors is not recommended.

Budek et al. (2000) recognized the importance of pile-tip deflection relative to pile-cap deflection when considering the topic of long-pile behavior. Budek attempted to establish a limit for long-pile behavior that was based on the proportionality of the pile-tip deflection to the pile-cap deflection under a specified load. The value of this ratio is largely influenced by the 0.0 deflection point for the pile tip, and has less to do with the pile-cap deflection. With a resulting pile tip depth of 52 ft (624 in.) for the 40 ft (480 in.) exposed section pile, which is very much deeper than the asymptotic pile-tip deflection slope per pile tip embedment inflection point method, this method is deemed to be conservative in estimating pile-tip depth for long-pile behavior. The additional pile depth of embedment requires more resources (time, material, etc.) for in-the-wet construction, increasing the costs without providing more capacity.

The authors prefer the asymptotic pile tip deflection slope per pile tip embedment inflection point method for determining the pile-tip depth for long-pile behavior because the inflection point can be determined accurately with the pushover peak loads. This inflection point also pinpoints the rate of change when the pile mobilizes the cohesionless soil due to variations in the p-y curves.

3 Summary, Conclusions, and Recommendations

Flexible, energy-resistant navigation systems, such as lock approach walls, founded on piles are a proven cost-effective technology for the Corps. Because of in-the-wet construction techniques and modular design, these systems can save millions of dollars as compared to the cost of rigid systems at installation and for remediation. As much as these systems save over traditional methods, additional savings can be achieved by minimizing the depth of embedment for the piles to guarantee long-pile behavior. This pile-depth minimization will maintain the structure's capability to withstand the loads that will be applied and allow minimal deflection.

The primary design load cases for pile-founded approach wall systems are when they are subjected to barge train impact events that act tens of ft above the mud line at a lock. These impact loads have peak forces in the hundreds of tons.

There are two primary types of flexible approach wall structures: impact decks, supported by several rows of piles, and impact beams simply supported on pile-founded bents. A pushover analysis can be performed for a cluster of piles that are in a line normal to the impacted face of the approach wall structure and, therefore, in line with the transverse load of the barge train during impact. For vertical pile structures, the pushover determines the capacity of the individual piles before hinging at the pile cap and hinging at a short distance below the mudline occurs. For the drilled-in-place reinforced concrete pile, the capacity at the pile cap differs from the capacity at a short distance below the mudline. Yielding of the pile occurs at the pile cap prior to yielding at a short distance below the mudline in the analyses discussed in this report. This pushover analysis provides the peak force that will affect the structure before the piles supporting the structure yield at a short distance below the mudline, leading to the imminent collapse of the structure.

In order to achieve mission objectives in a cost-effective manner, the Corps utilizes a performance-driven approach for the design of its structures. The design capacity of the structure is established for three load conditions and their probabilities, in conjunction with performance

criteria. A possible iterative design process was discussed in the first chapter of this report. The iterative process cycles through improvements in a pile-founded design with an excessive pile depth of embedment and pushover analysis of that design. The final design should meet, but not exceed, the Extreme Load Condition performance objectives established in Headquarters, U.S. Army Corps of Engineers (2004) to minimize costs. This design will generally meet the other load condition performance criteria (i.e., Usual and Unusual).

It is possible that other constraints will affect the design of these flexible structures, rather than performance objectives. For flexible structures that abut less flexible elements or support machinery, limits on deflection (referred to as "drift" in Werner 1998) and ductility may need to be included. For these circumstances, the pushover analysis may not be appropriate, and the Extreme Load Condition will need to be met within the deflection limits or ductility limits.

It is important to note that the pushover curves of Figures 2.9 and 2.22 are for a single pile. For a vertical pile structure with roughly equivalent piles, the actual force capacity for the entire structure given a deformation is found by scaling the vertical axis by the number of piles. For instance, for the two-pile example problem, the peak lateral load at the pile at which the 40 ft exposed pile of Figure 2.9 would achieve before mudline hinging would be 2*448 kips or 896 kips. The deflection of the structure at that load would stay the same at 28.9 in. (with long-pile behavior). This implies that a deflection or ductility limit could be established by increasing the number of piles in a system until the Extreme event load would cross the full system pushover curve at the specified limit.

In fact, there are at least three design methods for meeting deflection limits:

- Increasing the diameter of the pile,
- Using an impact deck instead of a pile bent with supported beam to take advantage of load sharing, and
- Introducing more piles into the system.

Increasing the reinforcement of the pile will not affect the deflection or ductility of the pile.

When conducting pile-to-soil interaction analyses using, for example, COM624G, the designer may want to consider the effects of cyclic loading on the pile-to-soil, p-y curves in the upper reach of the pile. This is because impact loadings for the lower-level impact events of the usual load case will be frequent and may result in softening of the p-y curve response within this zone. Softened p-y curves are sometimes referred to as cyclic p-y curves. Since the extreme load case will likely govern the vertical depth-of-pile embedment, and given this is an infrequent/rare impact event, it would likely be conservative to assign softened p-y curves along the entire length of the pile. It is not anticipated that usual load cases will induce cyclic load degradation in the lower reaches of the pile where there would be engagement under unusual and extreme barge impact load cases.

When this design is achieved, the pile depth of embedment can be determined. The design was accomplished using excessive pile depth of embedment during calculations to guarantee long-pile behavior. Long-pile behavior means that the pile will achieve a pushover mudline hinge collapse event with minimal deflection at the pile cap before the imminent collapse. With deeper embedment, the pile approaches long-pile behavior asymptotically. This implies that a minimal depth can be achieved that approaches the minimal pile-cap deflection associated with long-pile behavior.

Several state-of-practice methods exist in the pile design literature for the estimation of pile embedment to guarantee long-pile behavior. This report evaluated these methods and proposes a systematic method for determining a minimal pile depth of embedment in cohesionless (i.e., granular soil) that guarantees long-pile behavior for piles in a flexible approach wall system. The recommended procedure is referred to as the asymptotic pile tip deflection slope per pile tip embedment inflection point method and is used in conjunction with a pushover analysis.

This methodology centers on the use of the pushover analysis and especially the determination of the peak load for each increment of a clustered pile group occurring immediately before the flexural yielding of the vertical pile at the pile-cap connection to the bent and at a short distance below the mudline in a pushover analysis. These peak loads are applied to the structure to determine the deflections of the pile. For shorter pile-tip embedment depths, the pile does not yield; but, the soil yields under the load, allowing the pile to plough through the soil to

pushover. When this pile-tip depth of embedment exceeds the maximum depth for the soil-yielding behavior for the peak load, the computed top-of-pile deflection decreases asymptotically as the depth of the pile embedment increases until the deflection change is nominal. This inversely mirrors the deflections at the pile tip. The deeper depth of all of the incremental pushover loads establishes the pile-tip depth for the entire pushover analysis. Recall that long-pile behavior is defined by this nominal deflection change at the pile cap.

A systematic method for determining a minimal pile depth of embedment guaranteeing long-pile behavior is formulated based on observations from calculations made using the state-of-practice methods and an incremental pushover analysis that iterates over pile depth of embedment. The derivative curve of the change in deflection as the pile-tip depth increases also is also asymptotic, with an inflection point that occurs because of the cohesionless soil-yielding behavior.

Figure 3.1 revisits the derived values of pile-tip deflections versus change in pile-tip depth with respect to the pile-tip depth for the 40 ft (480 in.) exposed pile. An inflection point with pile-tip embedment at 42 ft (504 in.) is noticeable as the derived values change more rapidly when the pile tip embedment is under 42 ft than when the pile-tip embedment is over 42 ft. For this example, the inflection point occurs when the derived value of change in deflection per change in depth has a value of 0.01.

Figure 3.2 shows the deflections at the pile tip, mudline, and pile cap as the pile-tip depth increases for the 40 ft exposed pile. The area where the three curves show long-pile behavior is labeled. The results of the various state-of-practice, pile-depth procedures are displayed as well as the systematic approach favored by the authors.[1]

[1] This preferred procedure is referred to as the asymptotic pile tip deflection slope per pile tip embedment inflection point method, with its depth of embedment for long-pile behavior result identified in Figure 2.21 in the green box and arrow.

Figure 3.1. Derived values for change of pile-tip deflection for 40’ exposed pile.

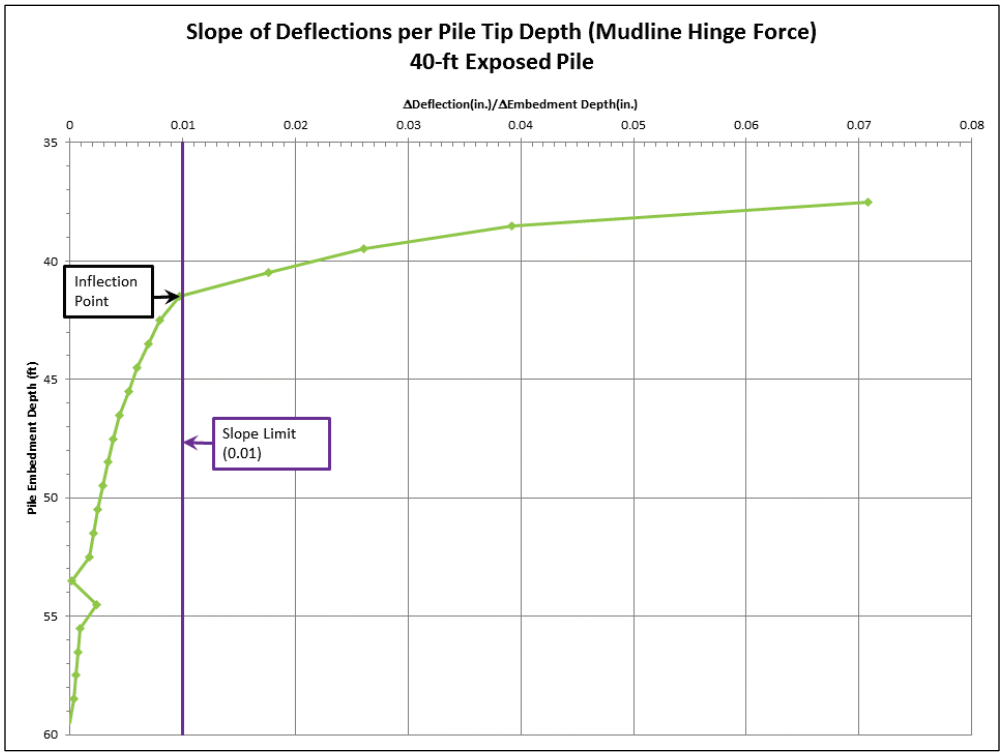

Figure 3.2. Comparison of methods for computing the pile-tip depth for long-pile behavior using Reese sand criteria results for 40’ exposed pile.

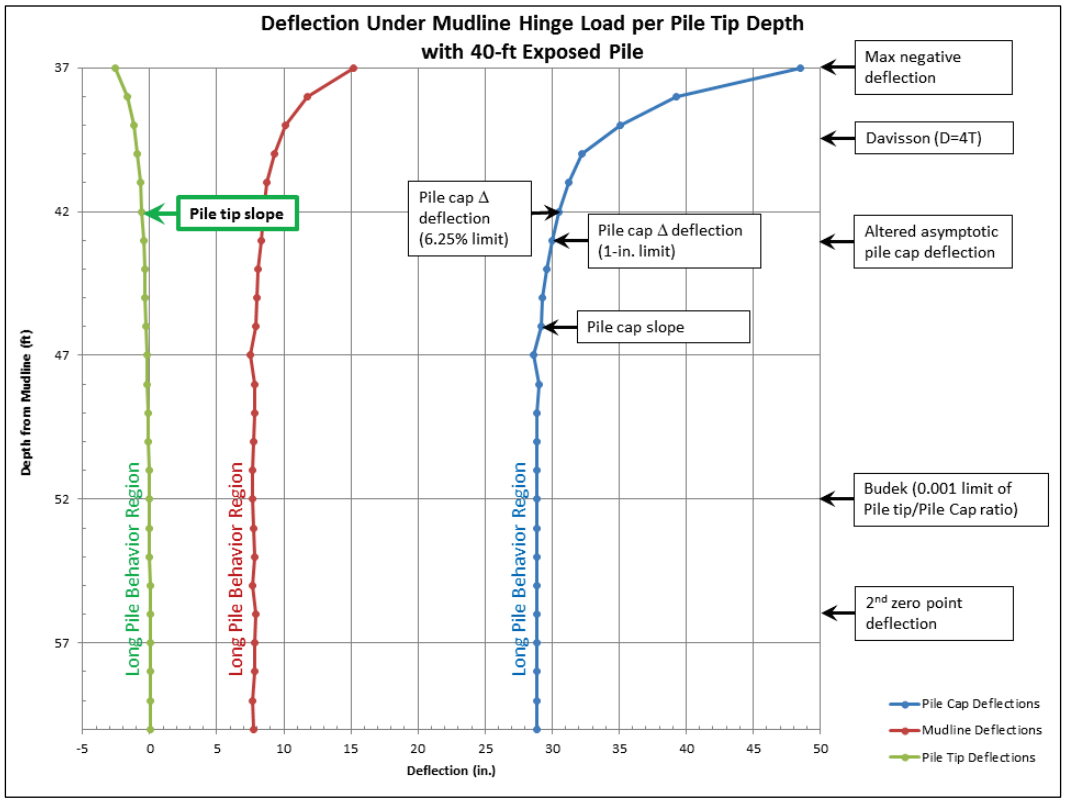

An additional example with the same properties for the cohesionless sand and pile, except for a shorter exposed pile height, was analyzed using the pushover capacity method. The shorter piles could withstand a higher peak impact load before mudline hinging and had smaller deflections. The peak load that the pile could withstand does not increase linearly with exposed height because of the change in internal pile-confining pressures due to slightly lower axial loading. The slightly lower axial loading occurs because of the loss of weight for the shorter exposed height pile.

The 20 ft (240 in.) exposed pile has lower deflections than its 40 ft (480 in.) exposed counterpart, but its asymptotic curve occurs at roughly the same pile-tip depths (as shown on Figures 3.1 and 3.3). However, the pile-tip depth at the inflection point for the 20 ft exposed pile was 2 ft below the pile-tip depth at the inflection point for the 40 ft exposed pile (44 ft (528 in.) as compared to 42 ft (504 in.) depth, respectively). This indicates that long-pile behavior is largely dependent on the cohesionless sand and pile properties other than the exposed length of the pile, but that the exposed length can affect the depth for a pile tip that will guarantee long-pile behavior.

Figure 3.3. Derived values for change of pile-tip deflection for 20' exposed pile.

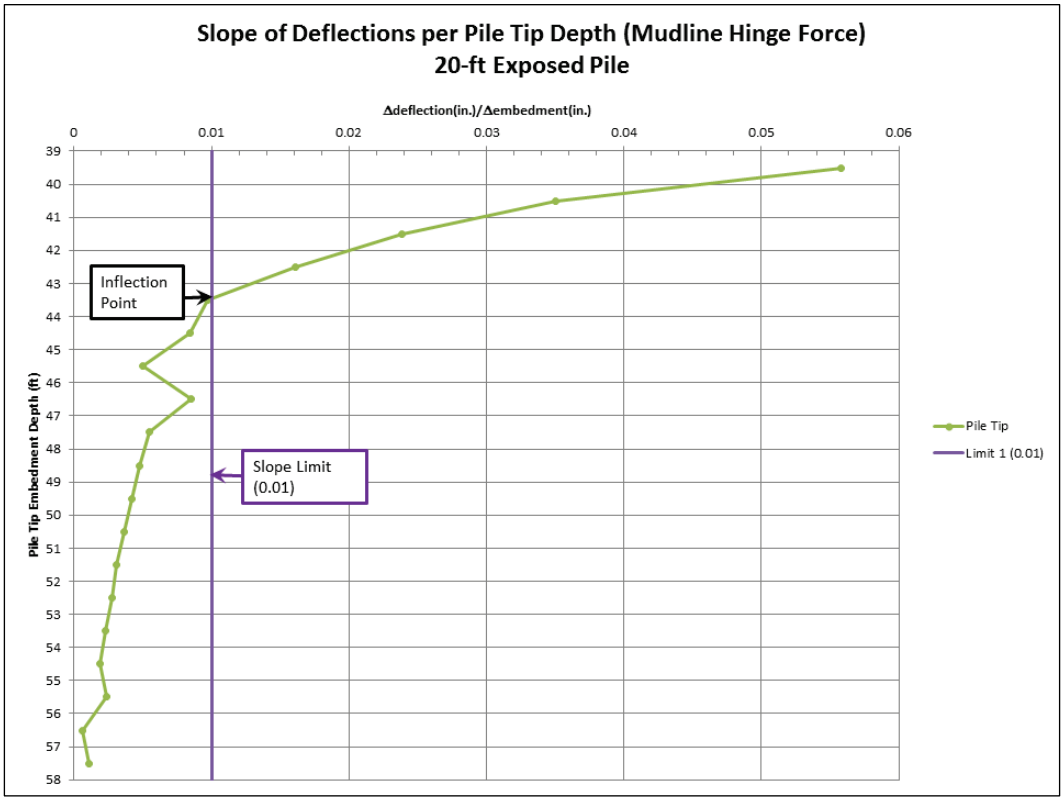

Figure 3.4 shows the deflections at the pile tip, mudline, and pile cap as the pile-tip depth increases for the 20 ft (240 in.) exposed pile. The area where the three curves show long-pile behavior is labeled. The systematic approach for determining the pile depth of embedment for long-pile behavior favored by the authors is also shown (with the result identified in Figure 3.4 by the green box and arrow).

Figure 3.4. Variation of deflections at pile tip, mudline, and pile cap for piles of varying depth using the Reese criteria for sand for a 20' exposed vertical pile.

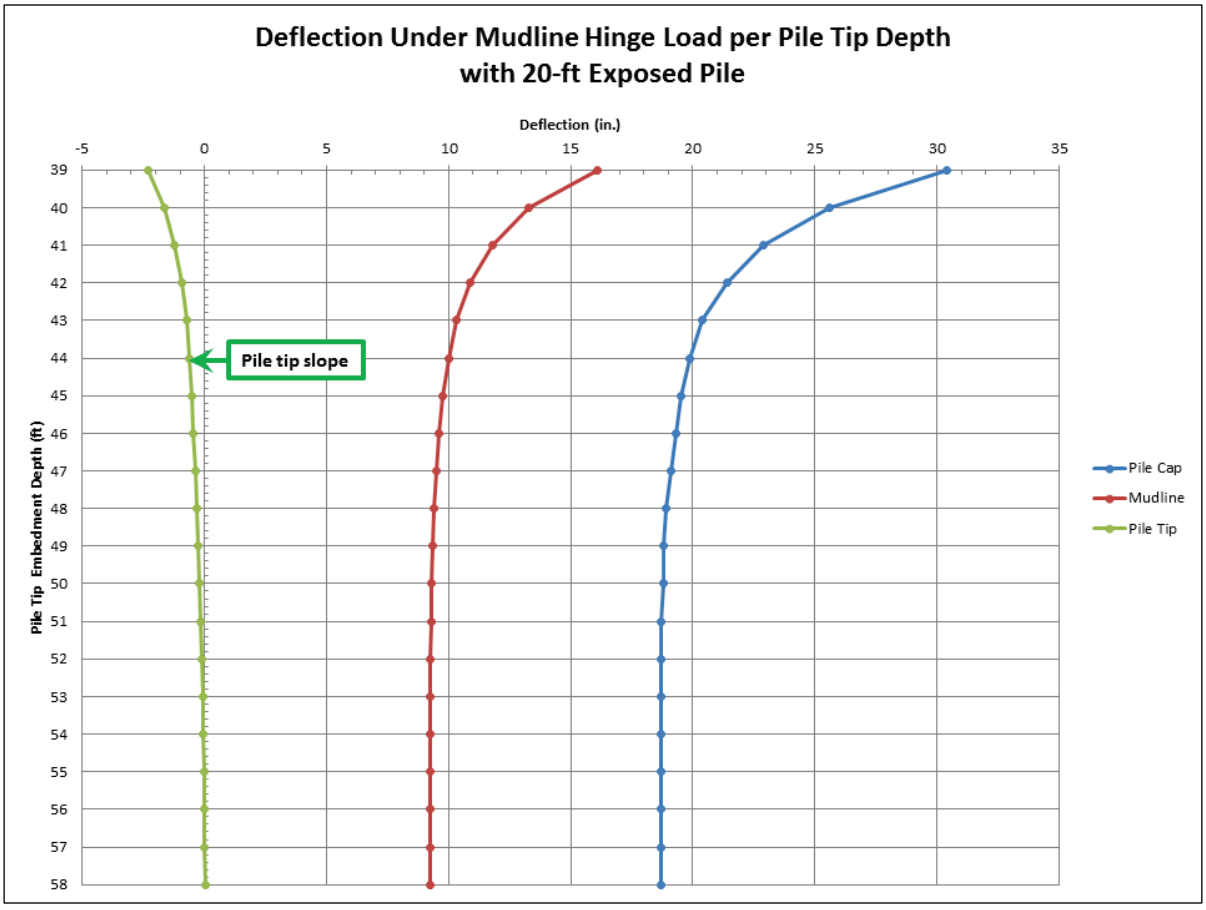

References

Broms, B. B. 1965. Design of laterally loaded piles. *ASCE Journal of the Soil Mechanics and Foundations Division,* 91 (SM3): 79-99.

Brown, D. A., J. P. Turner, and R. J. Castelli. 2010. Drilled shafts: Construction procedures and LRFD design methods. *Geotechnical Engineering Circular* 132014 (10), FHWA-NHI-10-016, Washington, D.C.: Federal Highway Administration.

Budek, A. M., J. N. Priestley, and G. Benzoni. 2000. Inelastic seismic response of bridge drilled-shaft RC Pile/Columns. *ASCE Journal of Structural Engineering* (April).

California Department of Transportation (CDOT). 1999. *Caltrans seismic design criteria, version 1.1*. Sacramento, CA: California Department of Transportation.

Castella, F., P. Martin, and J. Link. 1984. *Fixity of members embedded in concrete*. CERL TR M-339. Champaign, IL: U.S. Army Corps of Engineers, Construction Engineering Research Laboratory.

Davisson, M. T. 1970. *Lateral load capacity of pile groups*. Highway Research Record, Number 133, Pile Foundations. Washington, D.C.: Highway Research Board.

Ebeling, R. M., R. W. Strom, B. C. White, and K. Abraham. 2012. *Simplified analysis procedures for flexible approach wall systems founded on groups of piles and subjected to barge train impact*. ERDC/ITL TR-12-3. Vicksburg, MS: U.S. Army Engineer Research and Development Center.

Ebeling, R. M., B. C. White, and M. T. Fong. 2013. *Simulation and advance second moment reliability analyses of pile groups using CPGA-R*. ERDC/ITL TR-13-2. Vicksburg, MS: U.S. Army Engineer Research and Development Center.

Ebeling, R. M., B. C. White, B. C., and G. Galan-Comas. 2014. *Rotational Restraint of a 2V:1H Batter H-Pile to Lightly Reinforced Pile Cap Connection*. Project Report to New Orleans District. Department of the Army, Army Corps of Engineers, Vicksburg, MS: U.S. Army Engineer Research and Development Center.

Ebeling, R. M., B. C. White, A. Mohamed, and B. Barker. 2010. *Force time history during the impact of a barge train with a lock approach wall using Impact_Force*. ERDC/ITL TR-10-3. Vicksburg, MS: U.S. Army Engineer Research and Development Center.

Ensoft, Inc. 2004. *LPILE5 for windows*. http://www.ensoftinc.com/

Headquarters, U.S. Army Corps of Engineers (HQUSACE). 2005. *Stability analysis of concrete hydraulic structures*. EM 1110-2-2100. Washington, D.C.: U.S. Army Corps of Engineers.

Headquarters, U.S. Army Corps of Engineers (HQUSACE). 2004. *Barge impact analysis for rigid walls*. ETL 1110-2-563. Washington, D.C.: U.S. Army Corps of Engineers.

Headquarters, U.S. Army Corps of Engineers (HQUSACE). 1991. *Design of pile foundations*. EM 1110-2-2906. Washington, D.C.: U.S. Army Corps of Engineers.

Janoyan, K. D., J. P. Stewart, and J. W. Wallace. 2001. Analysis of p-y curves from lateral load test of large diameter drilled shaft in stiff clay. In *Proceedings, Caltrans 6th Seismic Design Workshop*, Sacramento, CA: Caltrans.

Janoyan, K. D., J. W. Wallace, and J. P. Stewart. 2006. Full-scale cyclic lateral load test of reinforced concrete pier-column. *ACI Structural Journal* 103 (2): 178-187.

Lien, B. 2011. Where is the fixity below top of an embedded laterally loaded pile or drilled shaft? In Proceedings, *6th Geotechnical, Geophysical and Geoenvironmental Technology Transfer (Geo3 T2) Conference and Expo*, Raleigh, NC: North Carolina Department of Transportation.

Park, H. 2002. *General guard wall design considerations for tow entry and exit*. ERDC/CHL CHETN-IX-8. Vicksburg, MS: U.S. Army Engineer Research and Development Center.

Reese, L. C., L. A. Cooley, and N. Radhakrishnan. 1984. *Laterally loaded piles and computer program COM624G*. Vicksburg, MS: Department of the Army, Army Corps of Engineers, Waterways Experiment Station, Technical Report K-84-2.

Reese, L. C., W. R. Cox, and F. D. Koop. 1974. Analysis of laterally loaded piles in sand. In *Proceedings, Offshore Technology Conference (OTC)*, Houston, TX: NRG Park.

Reese, L. C., M. W. O'Neill, and N. Radhakrishnan. 1970. Rational design concept for breasting dolphins. *Journal of Waterways and Harbours Division, Proceedings of the American Society of Civil Engineers* 96 (WW2) (May): 433-450.

Strom, R. W., and R. M. Ebeling. 2001. *State of practice in the design of tall, stiff, and flexible tieback retaining walls*. ERDC/ITL TR-01-1. Vicksburg, MS: U.S. Army Engineer Research and Development Center.

Wang, S-T, and L. C. Reese. 1993. *COM624P- laterally loaded pile analysis program for the microcomputer version 2.0*. Washington, D.C.: Federal Highway Administration, Office of Technology Applications, FHWA-SA-91-048.

Weatherby, D. E., M. Chung, N-K Kim, and J-L Briaud. 1998. *Summary report of research on permanent ground anchor walls; II, full-scale wall tests and a soil-structure interaction model*. McLean, VA: Federal Highway Administration, FHWA-RD-98-066.

Werner, S. D. 1998. Seismic guidelines for ports. *ASCE: Technical Council on Lifeline Earthquake Engineering* 12 (March).

Yang, N. C. 1966. *Buckling strength of pile*. Highway Research Record, Number 147, Bridges and Structures. Washington, D.C.: Highway Research Board.

Appendix A: On Using the Smeared Crack Material Model in COM624G

In this report, the pushover analysis was performed with CASE Library software COM624G, which maintains uniform properties for the entire pile, notably the EI term for stiffness. In a pushover analysis, extreme loading would occur to the pile, which would lead to moments inducing flexural yielding (hinging) of the pile. For COM624G, a smeared cracked EI term was used for the whole pile, assuming that the concrete had cracked for the length of the pile.

In reality, the pile will crack in regions where high moments occur and the pile has more freedom to rotate. It also reduces the incurred moments around that region. This implies that the deformations of a pile that starts uncracked and forms these cracked regions could have very different deformations than piles that assume that the pile has smeared cracked properties for its whole length.

The program LPILE by Ensoft, Inc. has capabilities to model the pile in the same manner of COM624G, but with cracked regions forming as a load is applied. The Chapter 2 example pile with 40 ft (480 in.) exposed height and 60 ft (720 in.) depth of embedment was input into LPILE for a pushover analysis. The results and comparison with COM624G are shown in Figures A.1-A.4.

Figures A.1 and A.2 show the deflection and moment comparison for the load in COM624G immediately before the pile cap hinging action with a lateral load at the pile cap of 367 kips. The cracked sections of the pile (in red) occur around the areas where hinging are assumed to occur; at the pile cap and at a short distance below the mudline. The deflections show that the uncracked sections of the pile provide some additional stiffness. The moment diagram is very similar between the LPILE and COM624G run. It is important to note that the flexural yielding has not yet occurred in the LPILE analysis.

Figure A.1. Comparison of deflections of smeared crack concrete properties and a model that propogates cracking along the pile using the load that instantiates pile-cap hinging in the smeared crack model.

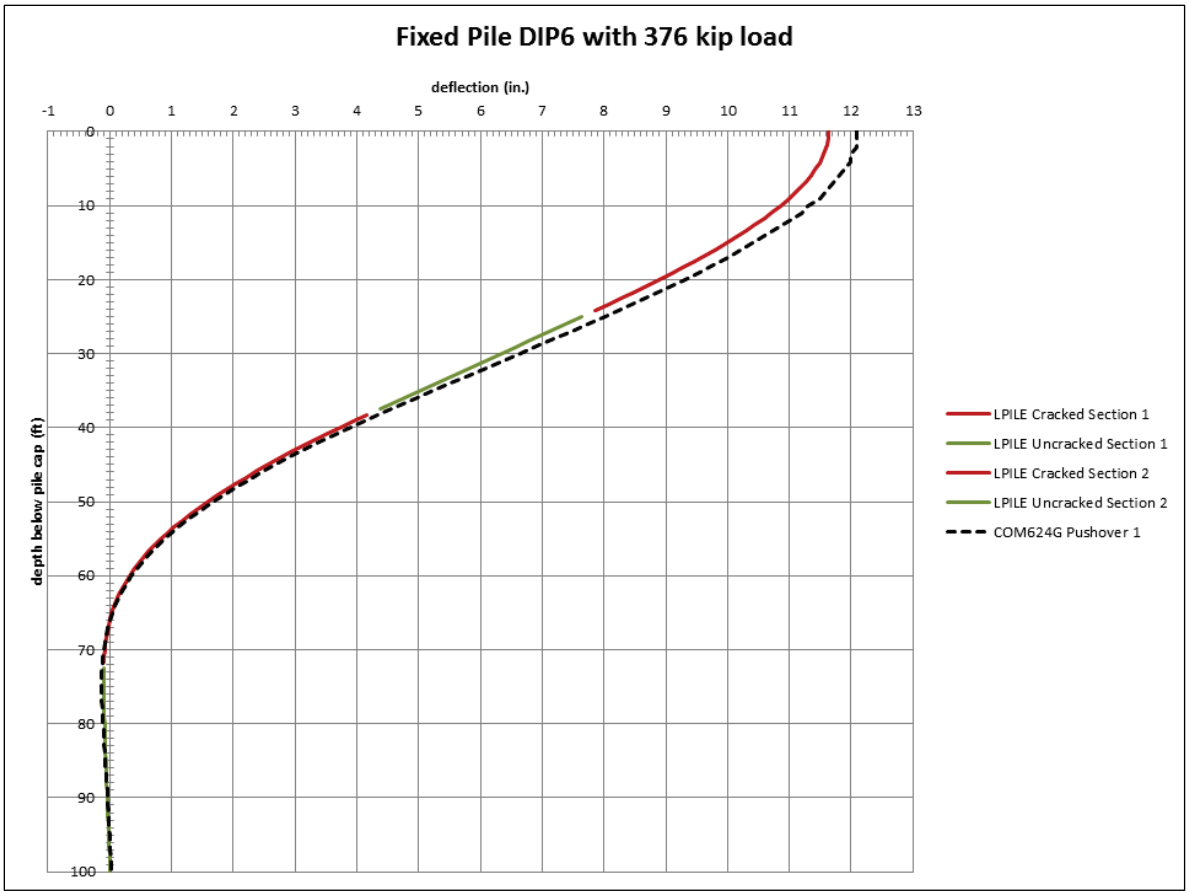

Figures A.3 and A.4 compare the deflections and moments for the smeared crack pile of COM624G and the LPILE pile at the point where both models have a lateral load that causes flexural yielding at the pile cap. For COM624G, this lateral load is 376 kips; for LPILE, this lateral load is 389 kips. The LPILE load has increased from the COM624G by slightly less than 4%, due to the stiffness of the uncracked regions in the pile. More notable is the fact that the deflection curves at the flexural hinging for both models are virtually identical. The moments vary, but only below the maximum moment within the embedded zone. The deflections in this lower region are minimal.

Figure A.2. Comparison of moments of smeared crack concrete properties and a model that propogates cracking along the pile using the load that instantiates pile-cap hinging in the smeared crack model.

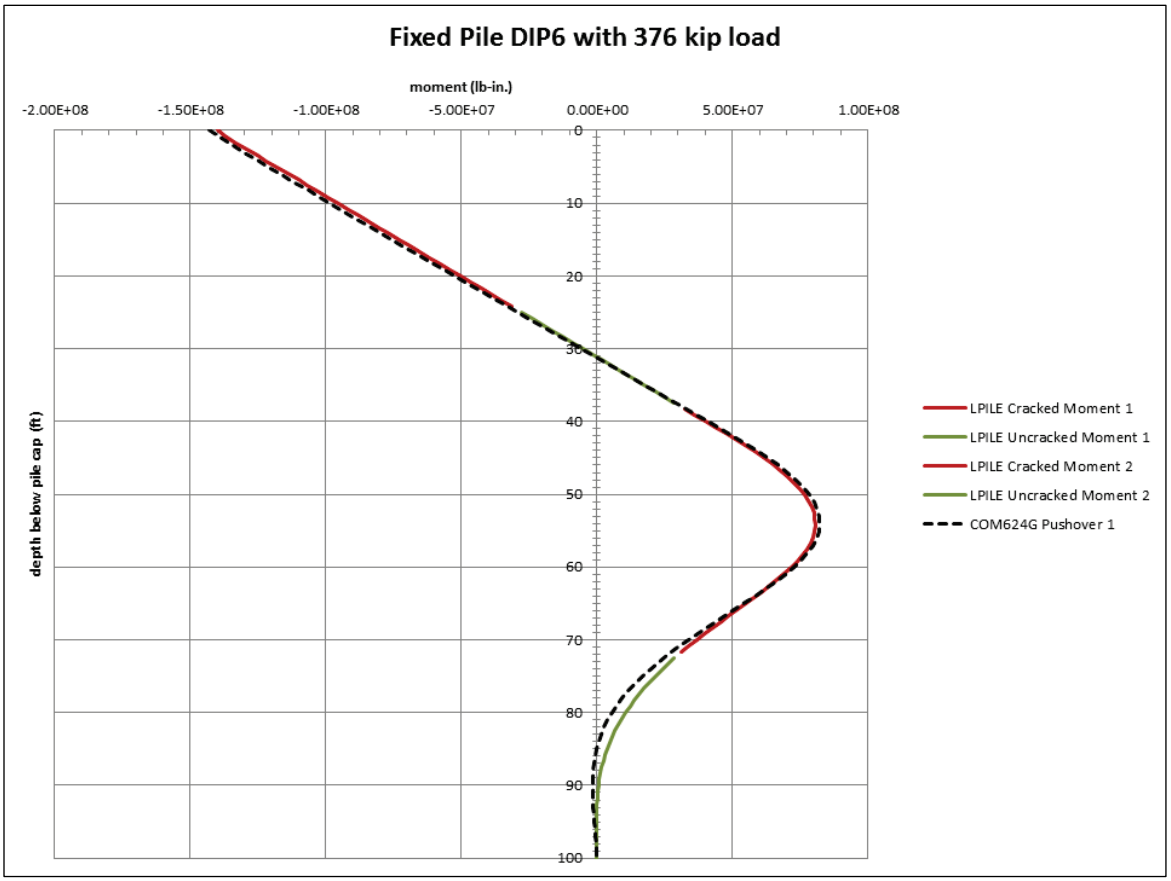

Figure A.3. Comparison of deflections of smeared crack concrete properties and a model that propagates cracking along the pile using pushover loads for each model.

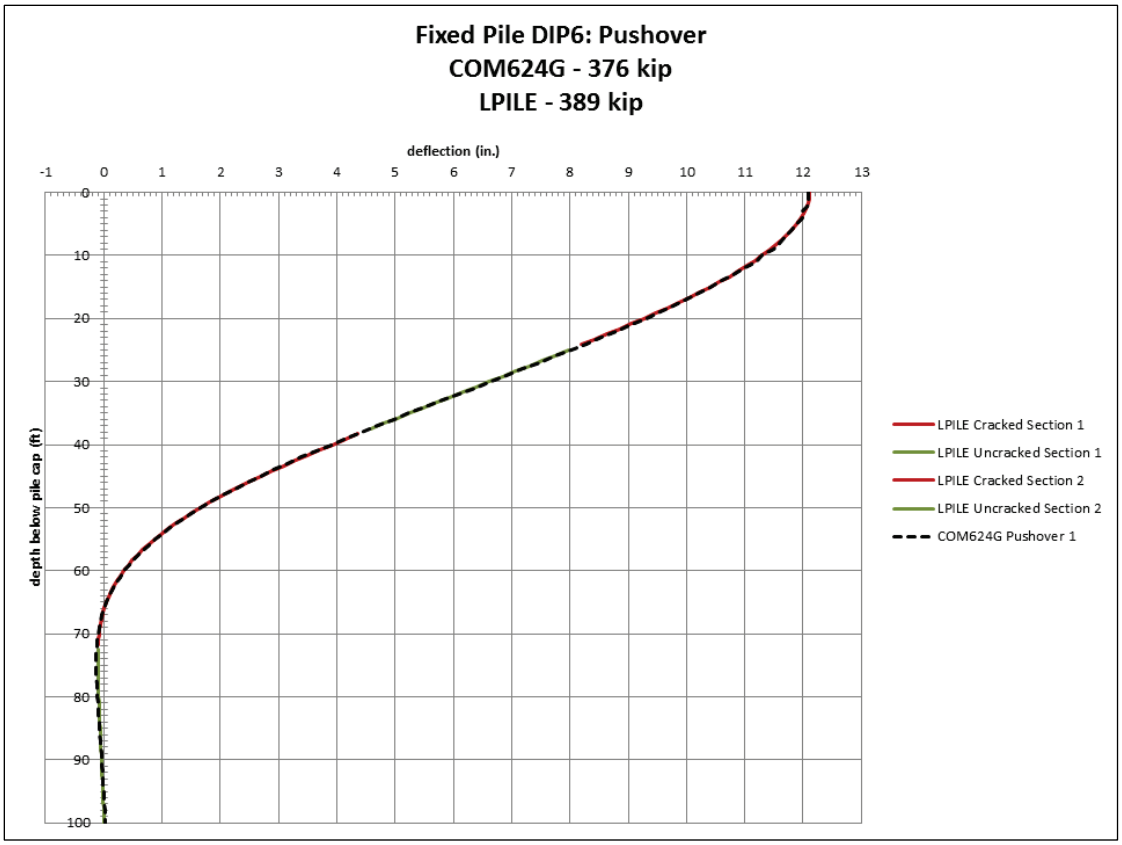

Figure A.5 shows the relationship between flexural stiffness and bending moment developing within the pile. For low bending moments the uncracked flexural stiffness value is assigned in the LPILE analysis. Once the cracking moment is exceeded, the cracked flexural stiffness is assigned in that region of the pile.

Figure A.4. Comparison of moments of smeared crack concrete properties and a model that propagates cracking along the pile using pushover loads for each model.

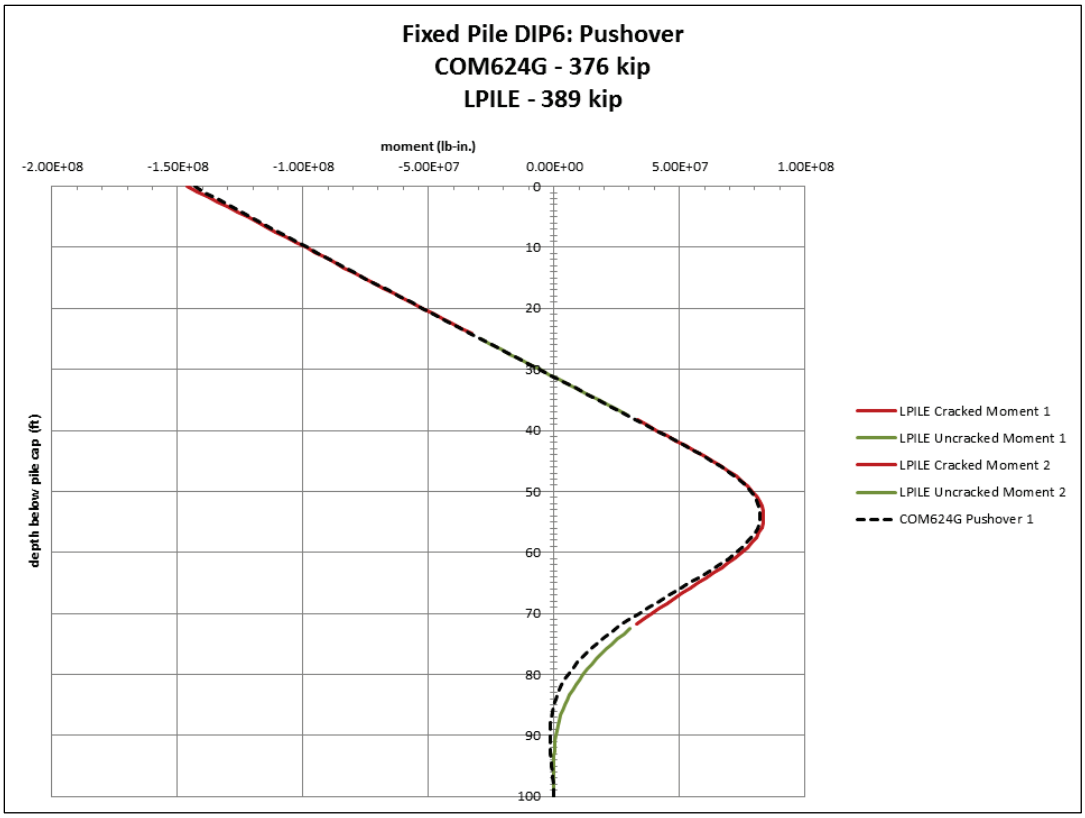

Figure A.5. Flexural stiffness versus bending moment.

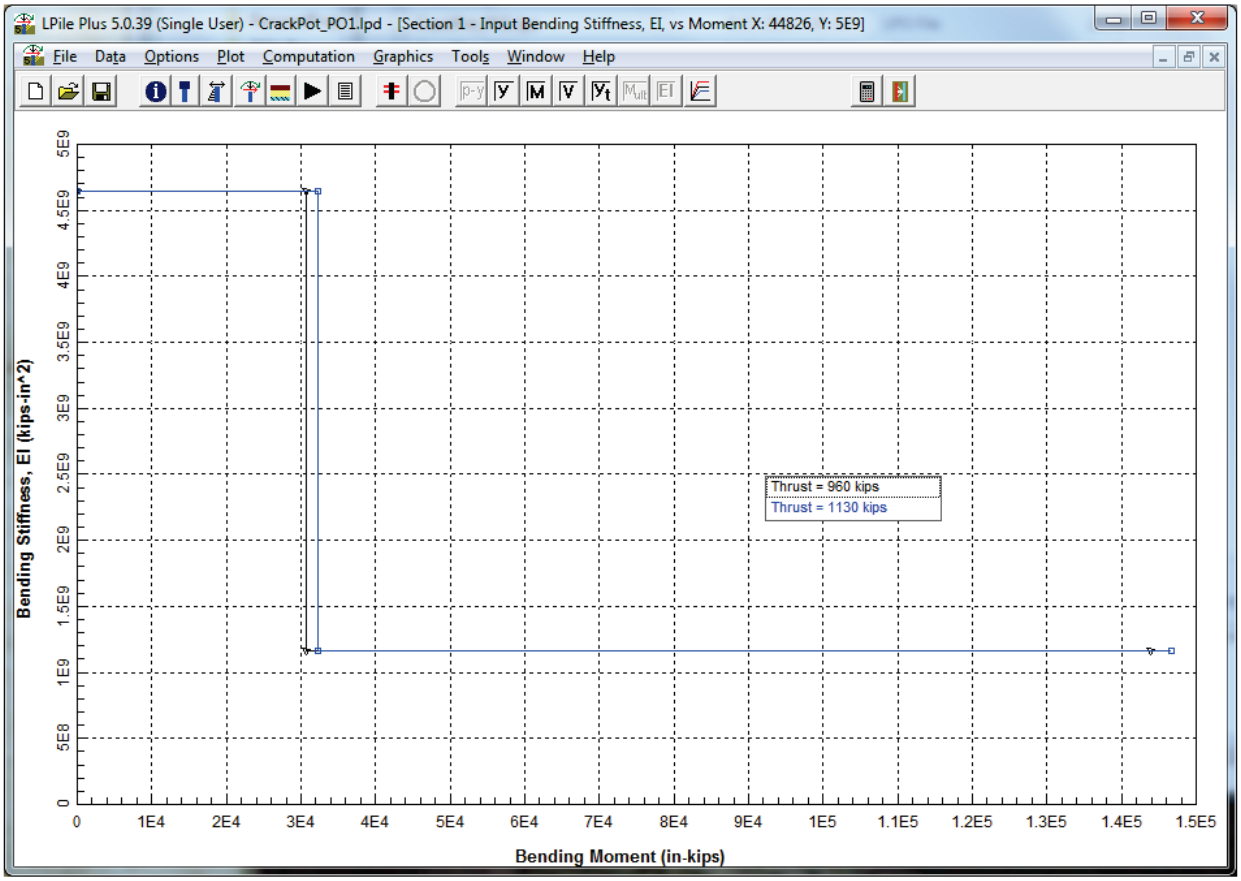

REPORT DOCUMENTATION PAGE

Form Approved
OMB No. 0704-0188

1. REPORT DATE *(DD-MM-YYYY)*	2. REPORT TYPE	3. DATES COVERED *(From - To)*
January 2017	TR	

4. TITLE AND SUBTITLE

A Systematic Approach for Determining Vertical Pile Depth of Embedment in Cohensionless Soils to Withstand Lateral Barge Train Impact Loads

5a. CONTRACT NUMBER

5b. GRANT NUMBER

5c. PROGRAM ELEMENT NUMBER

6. AUTHOR(S)

Barry C. White and Robert M. Ebeling

5d. PROJECT NUMBER
448769

5e. TASK NUMBER

5f. WORK UNIT NUMBER

7. PERFORMING ORGANIZATION NAME(S) AND ADDRESS(ES)

Information Technology Laboratory
US Army Engineer Research and Development Center
3909 Halls Ferry Road
Vicksburg, MS 39180-6199

8. PERFORMING ORGANIZATION REPORT NUMBER

ERDC/ITL TR-17-2

9. SPONSORING / MONITORING AGENCY NAME(S) AND ADDRESS(ES)

U.S. Army Corps of Engineers
Washington, DC 20314-1000

10. SPONSOR/MONITOR'S ACRONYM(S)

11. SPONSOR/MONITOR'S REPORT NUMBER(S)

12. DISTRIBUTION / AVAILABILITY STATEMENT

Approved for public release; distribution is unlimited.

13. SUPPLEMENTARY NOTES

14. ABSTRACT

Pile-founded flexible lock approach walls are typically constructed with impact beams simply supported on pile bents or by using an impact-deck supported by groups of clustered piles. Cast-in-drilled-hole (CIDH) reinforced concrete (RC) piles have seen recent widespread use as a cost-effective method of transferring superstructure loads to the foundation soil (e.g., cohesionless soils, like sand). The primary design load for lock approach walls are dynamic barge train impacts on a beam or deck which occur as the barge train aligns itself for entrance to the lock. These bents and decks are supported tens of feet (ft) above the mudline and barge impacts occur at the beam or deck level (i.e., lateral loading at approximately the top of the pile). Because of this lateral loading applied at the top of the piles, vertical pile groups must be designed to exhibit long-pile behavior (e.g., nominal change of deflection at the pile cap for a given load as the pile-tip depth-of-embedment increases). These design loads introduce substantial moments for the vertical piles at a short distance below the mudline. A pushover analysis of vertical-pile clusters can be performed to determine the energy absorption of the structure and the peak loads that cause the piles to hinge a short distance below the mudline, leading to collapse. This peak load is used to compare different pile depth-of-embedment procedures for long-pile behavior, and leads to the development of a new systematic procedure for defining this depth. Reducing the length of piles will result in a cost savings for Corps projects, especially for in-the-wet construction.

15. SUBJECT TERMS (see reverse)

16. SECURITY CLASSIFICATION OF:			17. LIMITATION OF ABSTRACT	18. NUMBER OF PAGES	19a. NAME OF RESPONSIBLE PERSON Robert Ebeling
a. REPORT	b. ABSTRACT	c. THIS PAGE			19b. TELEPHONE NUMBER *(include area code)*
UNCLASSIFIED	UNCLASSIFIED	UNCLASSIFIED	UNCLASSIFIED	81	6016343458

15. SUBJECT TERMS (concluded)

Barge impact
Barge train impact
Flexible lock approach wall
Flexible approach wall
Guide wall
Guard wall
Vertical pile groups
Clustered pile groups
Depth of embedment
Pushover analysis
Impact deck
Impact beam
Pile bent
Flexural yielding
Pile hinge
Elevated deck